



How to Design Donor–Acceptor Based Heterocyclic Conjugated Polymers for Applications from Organic Electronics to Sensors

K. Mahesh¹ · Subramanian Karpagam¹ · K. Pandian²

Received: 22 October 2018 / Accepted: 4 April 2019 / Published online: 22 April 2019
© Springer Nature Switzerland AG 2019

Abstract

Over the past few years, significant progress has been made in the design of organic semi-conducting conjugated polymers that readily transport holes or electrons and can result in light emission. The conjugated backbone consist mainly of electron-donating (donor) and electron-withdrawing (acceptor) units as alternating groups in a conjugated oligomer or polymer that can be regulated by physical properties such as π conjugation length, monomer alteration, inter/intramolecular interactions and energy levels. Certainly, it is notable today that the highest occupied molecular orbital level of the producing material is localized predominantly on the electron-donating moiety and lowest unoccupied molecular orbital level on the electron-accepting moiety. Conjugated oligomers or polymers are used in many detecting fields due to their exceptional ability to sense toxic chemicals, metal ions and bio-molecules. The conjugated polymers have unique delocalized π -electronic “molecular wires” that can expand the fluorescence intensity considerably. The fluorescence intensity of polymers can be quenched by particular quenching molecules. In this review, the fluorescence intensity, detecting of multiple metal ions, solubility, photochemical stability and optoelectronic properties of these conjugated polymers, and how they can be regulated by different functional groups, are discussed in detail.

Keywords Conjugated polymer · Inter/intramolecular interactions · Toxic chemicals · Fluorescence intensity · Optoelectronic properties

✉ Subramanian Karpagam
skarpagam80@yahoo.com

¹ Department of Chemistry, School of Advanced Science, VIT University, Vellore, Tamil Nadu 632014, India

² Department of Inorganic Chemistry, University of Madras, Guindy Campus, Chennai, Tamil Nadu 600025, India

1 Introduction

A polymer is a macromolecule or large molecule composed of many repeating monomer subunits connected covalently through polymerization. Because of their wide ranging properties, synthetic polymers play a significant role in daily life. The large molecular weights of polymers produce excellent physical properties such as semicrystalline character, toughness, tendency to form glasses and viscoelasticity. Polymers can be classified into different types depending on their physical and structural properties: linear, branched, hyperbranched, conducting, cross-linked, hetero and homopolymers, etc.

2 Conjugated Polymers

Conjugation is where systems of molecules contain delocalized electrons with alternating single and double bonds. Conjugation may lower the total energy of the molecule and enhance stability. In conjugation, π electrons behave differently as compared with sigma bond electrons. The largest examples of conjugated systems include carbon-based conductive polymers such as graphite, graphene and carbon nanotubes. Aromatic conjugated molecules follow Huckel's rule and display unusual stability. A typical example is benzene, which has six π -electron systems involved in conjugation. The π bonds of the P_z orbitals in benzene carbon atoms are perpendicular to the benzene plane and overlap with neighboring P_z orbitals. The semiconducting nature of the conjugated polymer depends on the delocalization of π -electrons [1].

Conjugated organic polymers act as semiconductors that conduct electricity due to the lower band gap. Their processability and dispersion nature are the major benefit of conjugated conductive polymers. They can deliver high electrical conductivity with different mechanical properties. Their electrical conductive properties can be tuned by advanced dispersion processes and organic synthetic methods [2]. Conventional polymers such as polyethylenes have low electron mobility and do not supply electrical conductivity due to sigma-bonding electrons. However, the situation in conjugated polymers is completely different because delocalized P_z orbitals increase electron mobility. Conjugated polymers have an energy band between 1.5 and 3.0 eV; due to this low bandgap, these polymers are employed broadly in photovoltaic devices, organic light emitting diodes (OLEDs), sensors, solar cells, organic thin film transistors (OTFT) and lasers.

2.1 Background and Scope of Conjugated Polymers

The first polycyclic aromatic compounds showing a semi-conducting nature due to halogens with charge-transfer complex were reported in the 1950s [3]. Elsewhere, Bell Laboratories reported low resistive ($8 \Omega \text{ cm}$) charge transfer complexes in 1954 [3]. In the 1970s, scientists reported metal-conductive

tetrathiafulvalene salts [4]. Although technically these compounds are not polymers, this demonstrated that organic molecules can carry current. In 1963, low resistive ($1 \Omega \text{ cm}$) polypyrrole derivatives were reported by Australian scientists [5]. Subsequently, high conductive polyanilines were reported in 1968 [6]. In 1977, Heeger and his team reported high conductive iodine-doped polyacetylene [7]. For this innovation, they were awarded the Nobel Prize in 2000. After the 1980s, OLEDs and photovoltaic devices were developed as a significant application of conjugated conductive polymers [8, 9]. Many excellent reviews, research papers, and patents have been published on conjugated polymers to promote these materials as promising for electroluminescent and optoelectronic applications [10–15].

2.2 Structure of Conjugated Polymers

The major categories of conductive polymers are linear backbones such as polyanilines, polypyrrole, polyacetylenes and their copolymeric derivatives. Poly(*p*-phenylene vinylenes) and their alkyl, alkoxy soluble derivatives have been developed as optoelectrical semiconducting polymers. Nowadays, poly(3-alkyl thiophene) are classical polymers for transistors and solar cells. The different polymer structures and their electrical band gaps and conductive values are shown in Table 1.

2.3 Properties of Conjugated Polymers

Conjugated polymers are capable of absorbing a broad range of sunlight because of atomic orbital interactions. Conjugated atomic orbitals exhibit single and double bond alterations along the entire conjugated polymer backbone. For example, the polyacetylene (Fig. 1) backbone consists of tetravalent carbon atoms. Of these, three electrons are engaged in framing three sp^2 -bonds between two carbon atoms, and one electron is involved in forming a bond between carbon and the adjacent hydrogen.

These bonds are positioned between two carbon nuclei, which produces a σ -bond nature. The *p*-orbital is left with one electron, which interacts with another adjacent *p*-electron from the nearby carbon atom. This leads to formation of highest occupied molecular orbital (HOMO) or π -bonding and lowest unoccupied molecular orbital (LUMO) or π^* -anti bonding; this then resolves further into a valence band (HOMO) and a conduction band (LUMO), which is closer to a conjugated polymer material. The energy contrast between HOMO and LUMO is illustrated as the energy band gap or band gap (Fig. 2).

The π -bonding orbitals of conjugated polymers are positioned out of plane. These orbitals reduce the photon energy due to the limited bound to the carbon atom which required for photoexcitation. Upon absorption of broad range photons, an electron jumps from the valence band to the conduction band, developing an exciton (bound electron–hole pair).

Table 1 Structures of conjugated polymers with their electrical properties. *LED* Light emitting diode


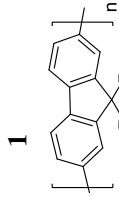
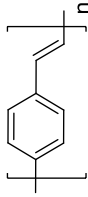
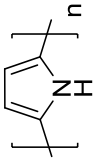
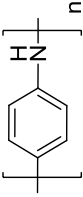
Polymer (date conductivity discovered)	Structure	Band gap (eV)	Conductivity (S/m)	Uses	References
<i>trans</i> -Polyacetylene (1977)		1.5	10^5	Organic conductor	[7]
Polyfluorene (1993)		3.2	10^4	Insulator	[16]
Poly(<i>p</i> -phenylene-vinylene) (1979)		2.5	10^{-3}	LEDs	[17]
Polypyrrole (1979)		3.1	10^2	Photoluminescence	[18]
Polyamine (1980)		3.2	10^{-9}	Electronic devices	[19]

Table 1 (continued)

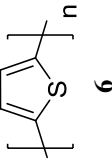
Polymer (date conductivity discovered)	Structure	Band gap (eV)	Conductivity (S/m)	Uses	References
Polythiophene (1983)	 <p style="text-align: center;">6</p>	2.0	$10-10^3$	Solar cells	[20]

Fig. 1 Schematic representation of the π -conjugated system in polyacetylene

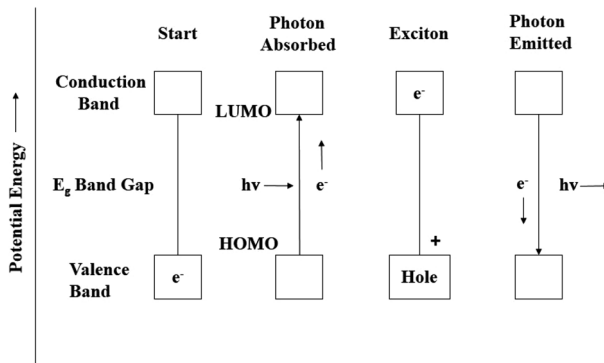
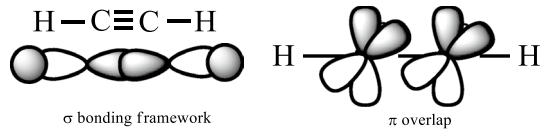


Fig. 2 Valance and conduction band, bordered by the highest occupied molecular orbital (HOMO) and lowest unoccupied molecular orbital (LUMO) energy levels, and separated by the energy bandgap and process of photoexcitation

2.4 Types of Conjugated Polymer

Variation in the conjugated backbone structure of polyacetylene, polythiophene, poly(*para*-phenylenevinylene)s, polythiazoles, polybenzothiadiazole has been shown to dramatically modify their electronic properties.

2.4.1 Polyacetylene

Polyacetylene is a conceptual structure derived from the polymerization of acetylene units to give a backbone chain with repeating ethylene groups $(\text{C}_2\text{H}_2)_n$. This compound is important for doping with Lewis acids and bases, which helps to increase conductivity, making it equivalent to metallic semiconductors. The highly dense polyacetylene is obtained using the Zeigler Natta catalyst. In 1970, homogeneous layers of polyacetylene were synthesized using titanium catalyst (an alternative to Ziegler Natta catalyst). Shirakawa and Heeger [21] discovered highly electrical conductive polyacetylene. This polymer attracted intense interest in the field of application of organic polymers in microelectronics (semiconductors) and its discoverers were awarded the Nobel Prize in 2000.

Exposing polyacetylene polymer films to the vapor of *p*-type dopants (electron accepting compounds) increases the electrical conductivity of the polymer over undoped polymers. These *p*-type dopants (Br_2 , I_2 , Cl_2 , and AsF_2) attract an electron from the polymer backbone and establish a charge transfer complex between *p*-dopant and polymer; this leads to increased conductivity. The

Table 2 *Cis* and *trans* orientation of polyacetylene

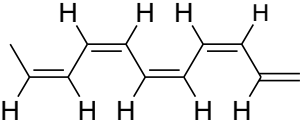
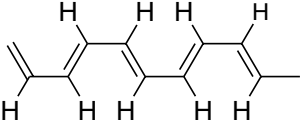
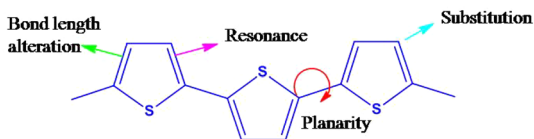
Polyacetylene	Structure	Conductivity
<i>cis</i> -Polyacetylene	 <p style="text-align: center;">7a</p>	$\sigma = 1.7 \times 10^{-9} \Omega^{-1} \text{ cm}^{-1}$
<i>trans</i> -Polyacetylene	 <p style="text-align: center;">7b</p>	$\sigma = 4.4 \times 10^{-5} \Omega^{-1} \text{ cm}^{-1}$

Fig. 3 Structural advantages of the polymer backbone of polythiophene

conductivity properties of polyacetylene depend on both the doping agent and the structure. Undoped *trans*-polyacetylene (7b) polymers possess a conductivity of $4.4 \times 10^{-5} \Omega^{-1} \text{ cm}^{-1}$, whilst *cis*-polyacetylene (7a) polymers possess a lesser conductivity of $1.7 \times 10^{-9} \Omega^{-1} \text{ cm}^{-1}$. This conductivity was increased to $0.5 \Omega^{-1} \text{ cm}^{-1}$ and $38 \Omega^{-1} \text{ cm}^{-1}$ after bromine, iodine doping. These conductivity values are represented in Table 2.

2.4.2 Polythiophene

In organic electronics, thiophene is one of the building blocks used most regularly due to its exceptional optical and electrical properties, and excellent thermal and chemical stability. Thiophene is also used widely in optoelectronic applications such as OLEDs and OTFTs. Polythiophene (homopolymer) was initially reported as a 1D-linear conjugated system in 1980 [22]. Polythiophene solubility is enhanced by the substitution of solubilizing units. Incorporation of heteroatom (substituents) to polythiophene alters the band gap via inductive and mesomeric effects. The structural advantages of the polymer backbone of polythiophene are shown in Fig. 3.

One of the biggest advantages of thiophene is its regioregularity. The three-substituted (asymmetry) thiophenes exhibited three probable couplings whilst two monomers are linked among the 2- and 5-positions shown in Fig. 4. The lower band gap and effective conjugation length depends on the regioregularity of thiophene. These particular couplings are:

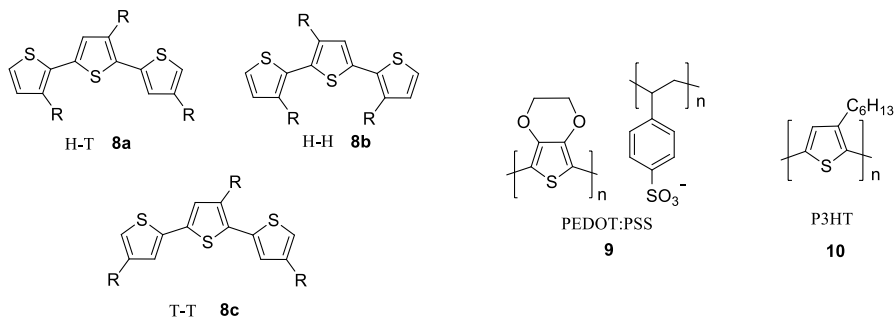


Fig. 4 Regioregularity of three-substituted thiophene and structures of poly(3,4-ethylene dioxythiophene) (PEDOT): poly(styrene sulfonate) (PSS) and poly(3-hexylthiophene) (P3HT)

- (1) Head to tail coupling (HT) or 2,5¹ coupling (8a).
- (2) Head to head coupling (HH) or 2,2¹ coupling (8b).
- (3) Tail to tail (TT) coupling or 5,5¹ coupling (8c).

Two thiophene-based conjugated polymers commonly found in the literature are poly(3,4-ethylene dioxythiophene) poly(styrene sulfonate) (PEDOT-PSS) (**9**) and poly(3-hexylthiophene) (P3HT) (**10**) (Fig. 4). PEDOT-PSS is applied widely as hole transport material in OLEDs and polymer solar cells. P3HT is used as a electron transporting substance (donor) in polymer solar cells. For example, thiophene derivatives such as thiophene-thienopyrazine based copolymer (**11**) exhibit a very low band gap and are used mainly in OTFTs due to their hole mobility nature [23]. The power conversion efficiency of thiophene-benzooxadiazole based polymer (**12**) was increased to 1.92% upon increasing the number of thiophene rings in the polymer backbone. New fluorene-*alt*-thienylene based polymers (**13**) exhibit multicolor luminescence because of different substituent position in thiophene rings and are mainly in electroluminescent devices (Table 3) [24].

2.4.3 Polybenzothiadiazole

2,1,3-Benzothiadiazole (BT) is an electron-accepting heterocyclic moiety that has been included with electron-rich species to construct a lower band gap for bulk heterojunction polymer solar cells. The electron-deficient nature of benzothiadiazole (**14a**) can be further improved by replacing the carbon atom with a *sp*²-hybridized nitrogen atom to produce aza-benzothiadiazole (**14b**) (Fig. 5). As well as a sulfur atom in benzothiadiazole unit can also be substituted for selenium is called a selino-benzothiadiazole (**14c**).

For example (see Table 4), the polymer (**15**) is the first candidate benzothiadiazole-based low band gap polymer to be prepared and applied in polymer solar cells [26]. The broad absorption peak of polymer **15** appeared at 775 nm in UV-vis absorption spectra, corresponding to the low band gap of 1.73 eV and this copolymer showed 7% of solar cell efficiency. The different ratios of thiophene and benzothiadiazole materials (**16**) showed distinctive optoelectronic properties [27]. Among

Table 3 Polythiophene-related conjugated polymers

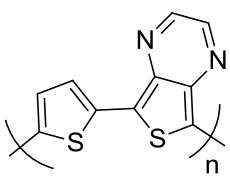
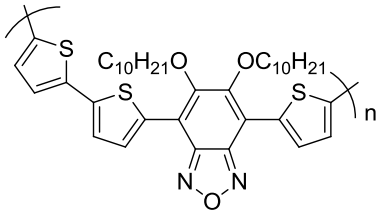
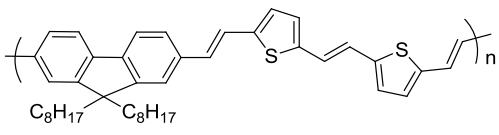
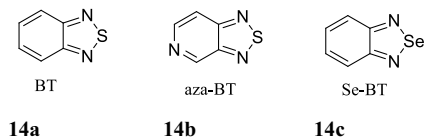
S. no.	Chemical structure	HOMO/LUMO	Band gap	References
1	 <p style="text-align: center;">11</p>	-4.45/-3.41	1.04	[23]
2	 <p style="text-align: center;">12</p>	-5.36/-3.63	1.82	[25]
3	 <p style="text-align: center;">13</p>	-5.50/-3.20	2.30	[25]

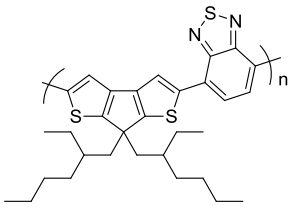
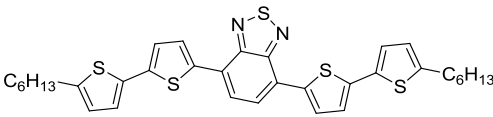
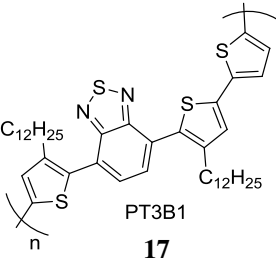
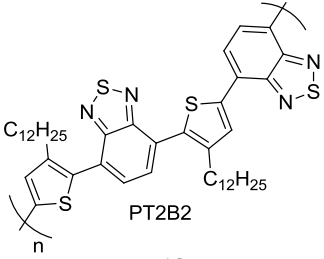
Fig. 5 Structures of benzothiadiazole, aza-benzothiadiazole, and selino-benzothiadiazole

these materials, four thiophenes and one benzothiadiazole molecule (**16**) showed 1.9 eV low band gap with high charge carrier mobility of $4 \times 10^{-3} \text{ cm}^2 \text{ V}^{-1} \text{ s}^{-1}$. Those materials have been optimized in OTFT devices. In addition, different ratios (3:1, **17** and 2:2, **18**) of thiophene- and benzothiadiazole-based push-pull copolymers showed red emission maxima at 618 nm (**17**) and 634 nm (**18**). Due to the high ratio of thiophenes, polymer **17** showed higher HOMO and lower LUMO values (Table 4) [14].

2.4.4 Poly(*p*-phenylenevinylene)

Poly(*p*-phenylenevinylene) (PPV) is one of the primary π -conjugated polymers due to its high photoluminescence and conductive properties. PPV was the first

Table 4 Polybenzothiadiazole-related conjugated polymers

S. no.	Chemical structure	HOMO/ LUMO	Band gap	References
1	 <p style="text-align: center;">15</p>	- 5.3/- 3.57	1.73	[26]
2	 <p style="text-align: center;">16</p>	5.15/3.25	1.90	[27]
3	 <p style="text-align: center;">17 PT3B1</p>	5.20/3.24 5.40/3.60	1.96 1.80	[14]
	 <p style="text-align: center;">18 PT2B2</p>			

conjugated polymer to be utilized as a part of polymer-based LEDs [28]. The highly efficient crystalline thin films can be processed by PPV polymers. Almost all PPV derivatives exhibit yellow fluorescence and have a small optical band gap, making PPV successful in light-emitting applications (LEDs). Moreover, its optoelectronic properties can be changed by substitution of functional side groups.

PPVs can be synthesized through various methods to regulate its molecular weight and purity. The most popular and versatile method is the Wessling and Zimmerman sulfonium precursor method shown in Fig. 6. Firstly, the bissulfonium intermediate salt was synthesized from α' -dichloro *p*-xylene, and was polymerized as

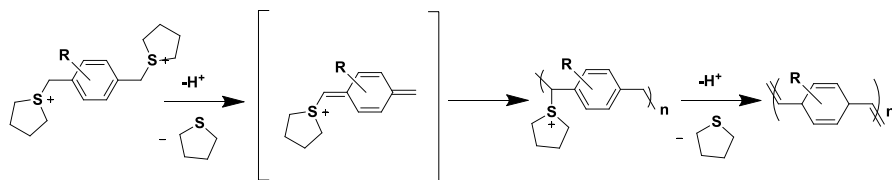


Fig. 6 Synthesis of poly(*p*-phenylenevinylene) (PPV) through the Wessling and Zimmerman sulfonium precursor method

PPV under mild basic and thermal condition. PPVs are highly crystalline in nature, thermally stable and mechanically strong due to their low solubility in atmospheric oxygen [29].

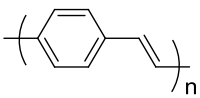
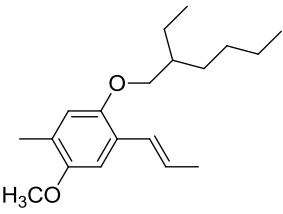
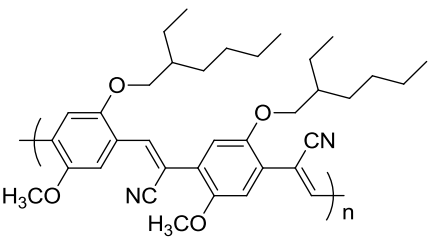
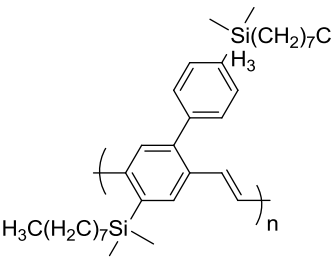
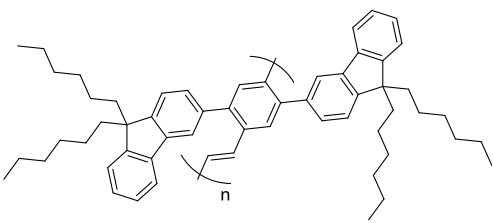
One of the biggest advantages of PPVs is the presence of alternative side-chains on the polymer backbone. PPV derivatives with a variety of substituents, such as alkoxy, phenyl, halide, silyl, fluorenyl, or cyano groups, have been reported. These many substituents have allowed the synthesis of different photoluminescence across the spectrum, such as blue, yellow, green, yellow-green, yellow-orange, red and red-orange. Examples of some substituted PPVs and their luminescence properties are listed in Table 5.

Unsubstituted PPVs (**19**) exhibit a lower HOMO value of -5.1 eV and a higher LUMO value of -2.7 eV, respectively. The corresponding band gap was calculated as 2.4 eV. After the introduction of alkoxy substituents on the phenylene ring, the band gap was reduced to 2.2 eV [30]. The energy band of the PPV derivative was tuned by adding substituents onto the vinylene linkages. These cyano-vinylene linkages lower both the HOMO and LUMO energy values. PPV derivatives with a cyano group substituted on the vinylene bond have been synthesized by Knoevenagel condensation, Wessling, and the Gilch route. Alkyl and alkoxy substituents of PPV increase the processability in the conjugation form and the cyano group increases the electron affinity of the polymer. Examples of a few PPV derivatives and their properties are discussed below based on previous literature.

Among PPV derivatives, thienylene-bonded PPVs show admirable optoelectronic properties. The random and alternative monomer of MEH-PPV and thienylene vinylene based polymer (**24**) (Fig. 7) were synthesized through Wittig-Horner condensation [31]. By increasing the number of thienylene vinylene units in the polymer backbone, the optoelectronic properties also increased. The optical absorption spectrum was red shifted by 20 nm. The oxidation value of polymer **24** was gradually decreased from 0.4 V to 0.08 V. The fill factor (FF) (42.6%) and short circuit current density (I_{SC}) (2.68 mA/cm²) were also decreased when compared with MEH-PPV (FF: 37.5% , I_{SC} : 2.09 mA/cm²).

Different poly(thiophene) substituted *p*-phenylenevinylenes have been synthesized with FeCl_3 [32]. The phenyl vinylene units are repeatedly in connection with two (**25**), four (**26**), and eight (**27**) thiophenyl moieties across the main polymer backbone (Fig. 7). The optoelectronic and thermal properties are elevated

Table 5 Poly(*p*-phenylenevinylene) (PPV)-related conjugated polymers

S. no.	Chemical structure	Emission color	Emission wavelength (nm)	HOMO/LUMO bandgap (eV)
1	 <p style="text-align: center;">19</p>	Green	550	-5.1 -2.7 2.4
2	 <p style="text-align: center;">20</p>	Red-range	610	-3.20 -5.40 2.20
3	 <p style="text-align: center;">21</p>	Red-orange	600	-5.50 -3.20 2.30
4	 <p style="text-align: center;">22</p>	Greenish yellow	495	-5.35 -2.86 2.49
5	 <p style="text-align: center;">23</p>	Green	485	-5.25 -2.76 2.49

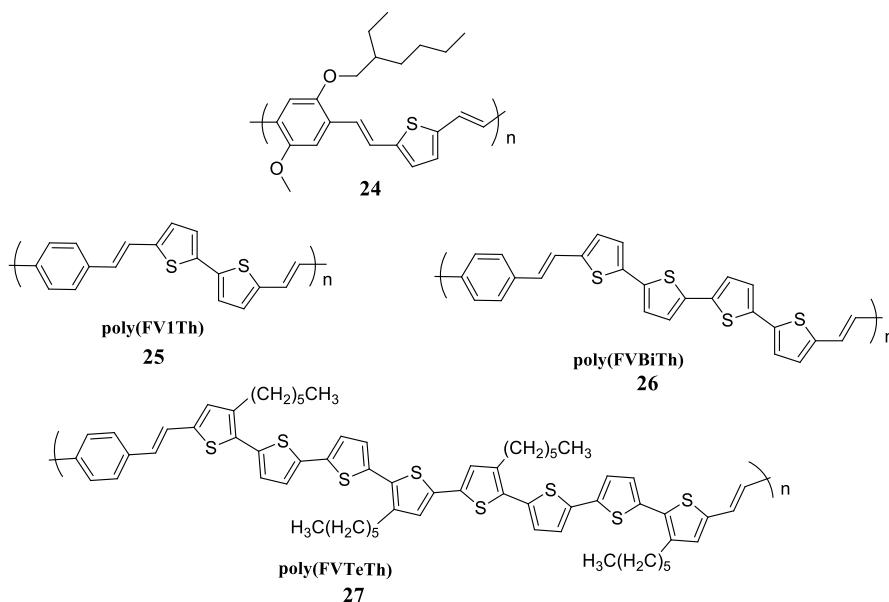


Fig. 7 Structures of various PPV-thiophene based conjugated polymers

as the number of thiophene rings in the polymer chain increases. Among the three polymers, **26** showed a lower HOMO value (-6.39 eV) and **27** showed a higher HOMO value (-6.12 eV) due to increasing number of thiophene rings. The polymer **27** has a lower band gap (2.31 eV) due to the greater number of alkyl substituted thiophene units.

2.4.5 Polythiazoles

In recent times, thiazoles containing conjugated polymers have been of enormous interest due to their optoelectronic applications. Thiazole is a familiar electron-withdrawing unit due to the presence of one electron-accepting nitrogen atom of imine ($-C=N-$) instead of a carbon atom at the third position of thiophene. Along with the sulfur atom in the thiazole ring, the nitrogen atom enhances the properties of conjugated polymers, which is attractive for photovoltaic applications. Moreover, thiazole-containing conjugated polymers acts as excellent fluorescence sensors for the identification of transition metal ions. Metal coordination of conjugated thiazole polymers can either increase or decrease fluorescence. Some examples of thiazole derivatives and their properties are discussed below based on previous literature.

Platinum (II) polyenes consisting of bithiazole-oligo(thienyl) ring-based polymers (**28**) (Fig. 8) show poor solubility due to polar soluble thiazole rings [33]. Due to the higher number of thiophene rings along with a strong withdrawing thiazole acceptor, P3 exhibits a higher HOMO value of -5.71 eV and the band gap is reduced to 2.06 eV.

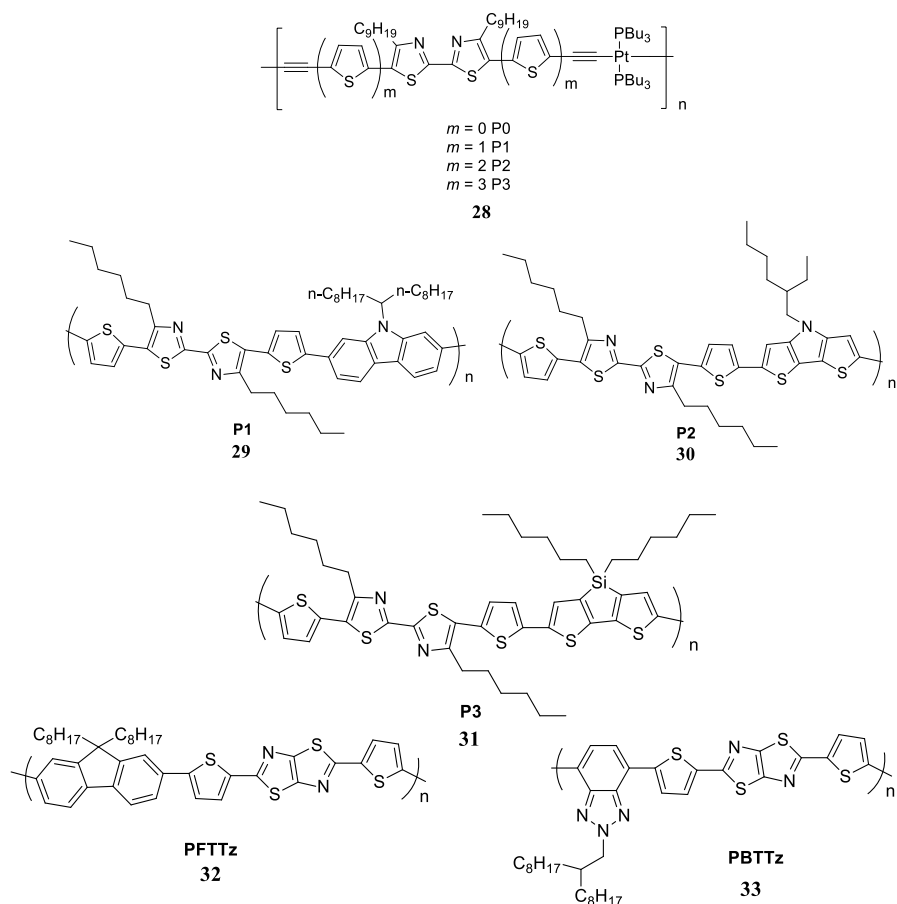


Fig. 8 Structures of thiazole-based conjugated polymers

Bithiazole acceptor and carbazole (**29**), dithienopyrrole (**30**), or dithenosilole (**31**) donor containing conjugated copolymers are synthesized through the Stille coupling reaction (Fig. 8) [34]. The donor–acceptor combinations used are very important to enhance optoelectronic and photovoltaic properties. Among these polymers, **31** has a similar absorption spectrum as P3HT, and higher absorption maxima in both solution and film (511, 558 nm) compared with other polymers. The electrical band gaps of **29**, **30**, and **31** are 2.53, 1.97 and 2.09. Obviously, the dithienopyrrole containing polymer showed a higher HOMO value (−4.76 eV) due to its high electron-rich nature, which will lead to a decrease in the open circuit voltage (V_{oc}).

The multichromic, solution processible and electroactive polymers **32** and **33** were synthesized via Suzuki and Stille coupling reactions [15]. Various linear and branched alkyl chains were substituted onto fluorene (**32**) and benzotriazole (**33**) polymers (Fig. 8). The similar HOMO value of −5.34 indicated that there is no influence of alkyl and branched chains on the polymer chain. Polymer **33** has lower LUMO (−3.19 eV)

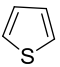
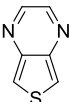
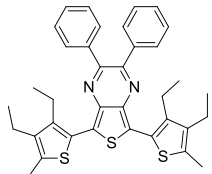
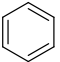
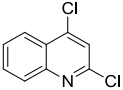
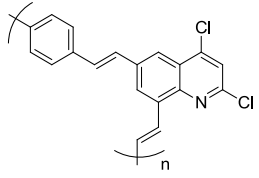
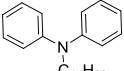
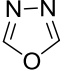
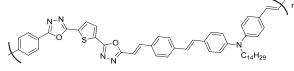
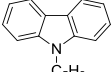
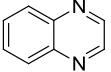
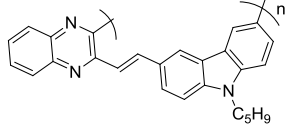
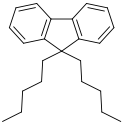
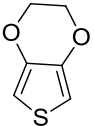
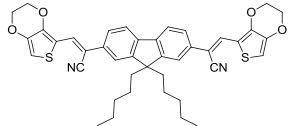
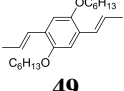
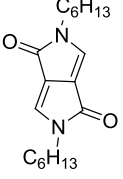
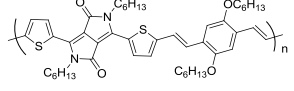
and band gap (1.79 eV) values when compared with **32** (−3.55 eV, 2.15 eV). The strong absorption and lower bandgap values of **33** should be useful for photovoltaic applications.

2.5 Donor–Acceptor Conjugated Polymers

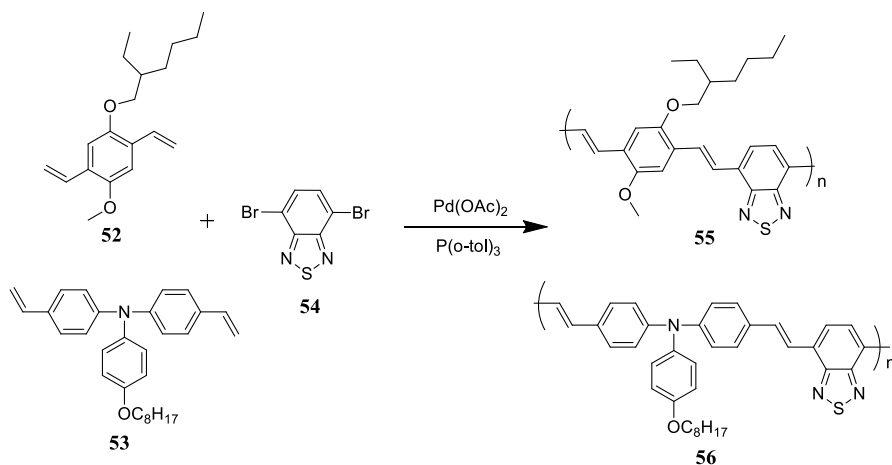
Electrochemical low band gap polymers can be synthesized through the incorporation of donor–acceptor units into the conjugated polymer backbone. This is another successful route to the synthesis of narrow bandgap polymers. This approach consists of a sequence of electron donating units (donor) and with electron accepting (acceptor) units. When compared to small molecules and metal complexes, donor–acceptor polymers are able to form continuous intramolecular charge transfer and intermolecular (through dipole–dipole interactions between donor and acceptor molecules on adjacent chains) interactions in the materials. This creates strong electronic coupling and closed π -stacking properties that enhance film crystallinity and charge transport efficiency. Moreover, conjugated polymers show better sensing performance than small molecules due to exciton migration along the conjugated chains. The energy levels of donor and acceptor moieties influence the band gap of the conjugated polymer. Moreover, the overall absorption energy of the polymer is increased by internal charge transfer between donor and acceptor units [35]. The delocalization of π -electrons in the entire conjugated chain may also lead to a lower bandgap; this approach was first proposed in 1993 [36]. The combination of donor–acceptor units in polymer improves the development of the mesomeric quinoid structure ($D-A \longleftrightarrow D^+=A^-$), over the initiation of a push–pull strategy that significantly lowers the band gap value. The band gap of conjugated polymers is resolved by the energy value of the LUMO of the acceptor moiety and the HOMO of the donor moiety. The lower bandgap of the polymer is influenced by the effect of low energy of LUMO and higher energy of HOMO [37, 38]. The band gap is also reduced by increasing the the conjugation length of donor–acceptor units. Conjugation of the polymer backbone can reduce the torsion angle by increasing the planarity [39].

Donor–acceptor based conjugated polymers consist mainly of three groups: (1) conjugated backbone, (2) substituents and (3) side chains. The band gap reduction and photophysical properties are very dependent on the conjugated backbone, which is composed of electron donors and acceptors. The donor–acceptor substituents can influence the nanostructure morphology and energy levels. Side chains, such as long alkyl or alkoxy chains, increase the molecular weight, solubility, and processability for large-scale processing and also increases the HOMO energy level due to their electron-donating nature [40, 41]. There are many electron-donating moieties, such as thiophene, phenylenevinylens, carbazole, pyrrole, fluorene and triphenylamine moieties with different substituents that enhance the optical and electrical properties. The various acceptor units such as thiazole, quinoline, benzothiadiazole, pyrazine, oxadiazole, and diketopyrrolopyrrole can be used to improve conductivity through lowering of the LUMO value. These donor and acceptor units were combined into one backbone through the different polymerization techniques.

Table 6 Different types of donors and acceptors in the conjugated backbone and their properties

Donor	Acceptor	E_g^{opt}	E_g^{cl}	T_d	References	Polymer
 34	 35	1.60	1.63	138	[42]	 36
 37	 38	2.54	2.55	470	[43]	 39
 40	 41	1.09	2.1	300	[44]	 42
 43	 44	2.20	2.26	325	[45]	 45
 46	 47	1.88	1.92	–	[46]	 48
 49	 50	1.94	1.93	256	[47]	 51

Some examples of donors and acceptors with their properties are shown in Table 6. Polymer **36** is synthesized from thiophene donor (**34**) and **35** by Suzuki coupling. Polymer **36** exhibits broad absorption spectrum from 350 to 950 nm,



Scheme 1 General synthesis of Mizoroki–Heck coupling reaction

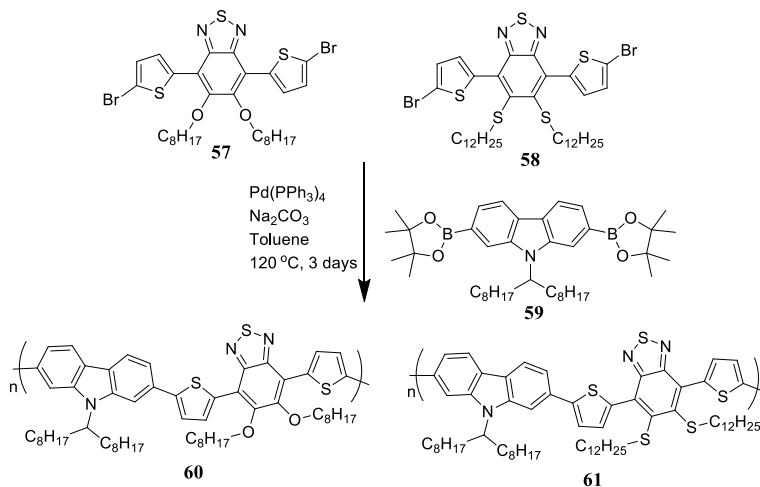
and has good stability and solubility. Oligomer **39** is synthesized from **37** and **38** by a Wittig condensation route. The absorption value of **39** is at 382 nm and it exhibits bluish green emission maxima at 477 nm. The higher thermal stability of 470 °C is due to the quinoline (**38**) moiety. Polymer **42** was synthesized from diphenylamine donor (**40**) and oxadiazole acceptor (**41**) through a Wittig condensation reaction. Polymer **42** shows absorption at 446 nm and emission at 532 nm in chloroform solution. Due to the strength of diphenylamine (**40**), the band gap is significantly decreased.

2.6 Synthesis of Conjugated Polymers

Based on polymerization techniques, it is possible to differentiate three main types of reaction: polycondensation (step-growth), polyaddition and chain polymerization. Monomers are consumed rapidly in polycondensation and polyaddition due to decrease in polymerization rate. Stoichiometric amount of the two monomers affect the final molecular weight of the polymer. The higher molecular weight of the polymers are increased mainly by the purity of the monomers. Conjugated polymers are synthesized mainly by polycondensation reactions using the various routes such Mizoroki–Heck, Suzuki–Miyaura, Stille coupling, and Wittig condensation reactions. These polymerizations proceed by two different monomers and are catalyzed by palladium [Pd(0)].

2.6.1 Mizoroki–Heck Coupling Reaction

The polymerization of *bis*-aryl halides and alkene derivatives to generate photovoltaic materials with high conductive, optoelectrical and luminescent materials are called Heck coupling reactions. Classical Heck conditions require a reducing agent

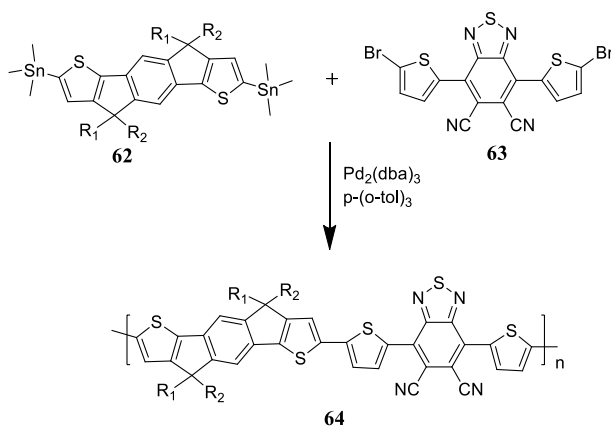


Scheme 2 General synthesis of Suzuki–Miyaura coupling reaction

(triphenylphosphine), high temperatures and palladium catalyst ($> 120\text{ }^{\circ}\text{C}$). Of all polymers, block copolymers are widely synthesized through the Heck coupling reaction. For example, electron-rich alkoxy substituted *p*-phenylene vinylene (PPV) (**52**) or triphenylamine (TPA) (**53**) vinylene and electron-deficient bromo-substituted 2,1,3-benzothiadiazole (**54**) polymerize in the presence of $\text{Pd}(\text{OAc})_2$ as a catalyst and tri(*o*-tolyl)phosphine as a reducing agent (Scheme 1) [45]. Of these polymers, PPV based polymer **55** showed a lower optical band gap value (1.76 eV) than the TPA-based polymer **56** (1.86 eV) due to the long conjugation length. In fact, TPA based polymer (**56**) conjugation is disrupted by the nitrogen of the amine group. The Heck-synthesized coupled polymers are applied successfully in photovoltaic devices.

2.6.2 Suzuki–Miyaura Coupling Reaction

The palladium-catalyzed cross-coupling reaction between alkenyl boranes and aryl halides is called the Suzuki coupling reaction and it was first reported in 1979. It is a controlled method for the formation of sp^2 hybridized C–C bonds, and a successful polymerization method due to many advantageous characteristics, such as the easily handled, organoborane starting materials, which are moisture- and air-stable. This method releases less-toxic inorganic materials as byproducts when compared with the toxic Stille polycondensation reaction. Moreover, it is a stereospecific, convenient and requires mild reaction conditions, as well as being regioselective and affording large freedom in selection of functionality. Thus, the Suzuki–Miyaura reaction is especially helpful for industrial applications. For example, carbazole and thioalkyl (**61**), alkoxy (**60**) substituted benzothiadiazole-based polymers are synthesized through the Suzuki coupling reaction (Scheme 2) [48]. Different electronic properties were observed through the incorporation of thioalkyl and alkoxy groups. The thio group of polymer **61** leads to enlarging Stokes shift up to 224 nm.



Scheme 3 General synthesis of the Stille coupling reaction

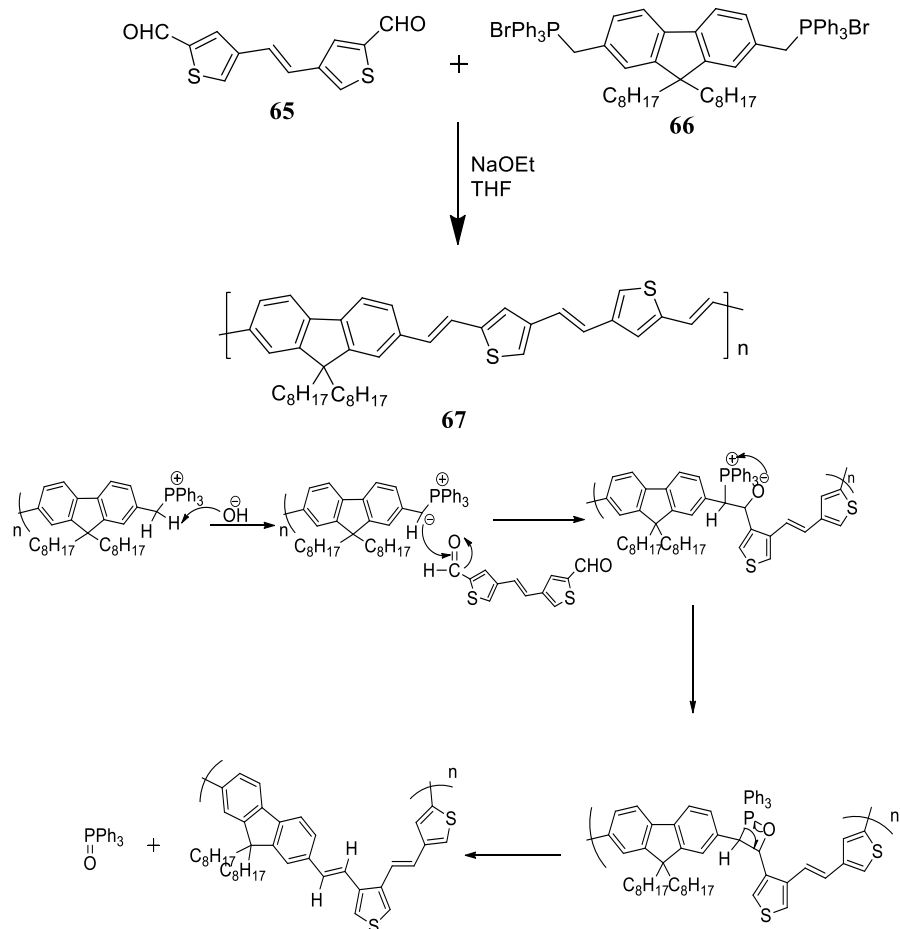
The photovoltaic efficiency of **60** is almost double (PCE: 4%) when compared to **61** (2%).

2.6.3 Stille Coupling Reaction

The C–C coupling between stannanes and aryl halides in the presence of palladium catalyst is called the Stille coupling reaction. It is a versatile synthetic reaction and has been commonly used for the synthesis of various organic compounds and polymers. It has numerous advantages, as it is regioselective, stereospecific and classically gives exceptional yields. It can proceed with multifunctional groups and it requires only a mild reaction environment. The first polymerization of dihalide and organo stannanes monomers were reported in the 1980s. Stille coupling based polymerization is used widely in thiophene-based monomers. The indacenodithiophene (**62**)-based donor and cyano-substituted benzothiadiazole (**63**)-based acceptor was polymerized through the Stille coupling reaction, catalyzed by $\text{Pd}_2(\text{dba})_3$ and reduced by $P\text{-(}o\text{-tol)}_3$ (Scheme 3) [50]. The synthesized polymer (**64**) exhibited a reduced optical band gap of 1.4 eV and an electrochemical band gap of 1.67 eV and is used to investigate charge mobility in OTFT devices.

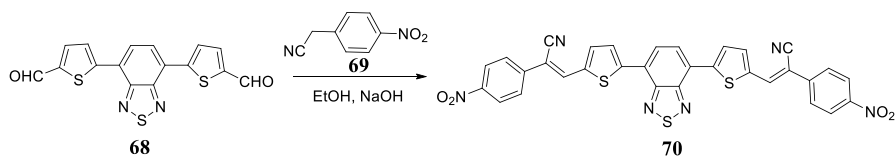
2.6.4 Wittig Condensation Reaction

The generation of carbon–carbon double bond (alkenes) from aldehydes and phosphorous ylides is known as the Wittig reaction. Since its innovation, the Wittig reaction has developed into one of the most effective and important methods for the synthesis of olefins. Phosphorous ylide is one of the active reagents in this reaction, and is generally synthesized from a triphenylphosphine and primary or secondary alkyl halides followed by a suitable base (e.g., NaH, NaOR, RLi etc.) for deprotonation. Based on the alkyl substituents on ylide, three classes can be differentiated: (1) ylide containing an alkyl substituent having at least one strong electron deficient group is



Scheme 4 General synthetic reaction and mechanism of Wittig reaction

called stabilized ylide, which stabilizes the electron-rich nature of the carbon; (2) ylide alkyl substituents with at least one alkenyl or aryl groups, which are less stable carbon, are called semi-stabilized ylide; and (3) ylide containing only alkyl group, which does not stabilize the carbon atom, are called nonstabilized ylide. The *E* or *Z*-stereoselectivity of the formed product is influenced by many factors, such as the type of aldehyde, type of ylide, nature of the solvent medium, and the counter ion for the phosphorous ylide generation. For example, the diphenylphosphonium salt of fluorene (**66**) and thiophene dialdehyde (**65**) undergo Wittig polymerization in the presence of sodium ethoxide (Scheme 4) and those polymers were used in electroluminescent devices [24].



Scheme 5 General synthesis of Knoevenagel reaction

2.6.5 Knoevenagel Condensation

The reaction between active methylene group containing molecules and aldehydes in the presence of a base to afford α,β -unsaturated compounds is known as Knoevenagel condensation. The active methylene compounds should have two electron-withdrawing groups. Water is the by-product of the reaction and is separated from the reaction by means of azeotropic distillation or the addition of molecular sieves. The major advantage of this reaction is that the synthesized major product is thermodynamically more stable. For example, the benzothiadiazole based aldehyde (**68**) was reacted with active methylene containing 4-nitrobenzyl cyanide (**69**) in the presence of sodium hydroxide. The resulting compound (**70**) exhibited high thermal decomposition temperature of 450 °C (Scheme 5) [50].

2.7 Applications of Conjugated Polymers

Conjugated semiconducting small molecules, oligomers and polymers have been vital materials in the development and progress of flexible and printable electronics. These semiconducting materials have attracted much attention over the last 20 years for several electronic device applications, such as OLEDs, organic photovoltaic and organic thin film transistors, as well as biological and chemical sensors due to their adjustable optical and electrical properties.

2.7.1 Organic Light Emitting Diodes

The emissive electroluminescent layer of OLEDs emits light in response to an electric power. A current goal of optoelectronic applications is to replace conventional light sources, such as fluorescent and incandescent lighting, with much more power-efficient light sources, is already making an impact in this industry. The advantages of LED lighting include self-sustainability, lower monitoring, and lower fire risk. OLEDs can be seen to be evolving to become an alternative to LEDs in emission applications, and will ultimately replace LCD display technology. Conjugated polymers are great innovative materials for the development of OLEDs due to their tunable emissive colors, which can be altered by structural adjustment. In device fabrication, the emissive conjugated polymer film is coated between two electrodes. Transparent indium tin oxide (ITO) glass plates are used as the anode and Al, Mg or Ca metals are used as the cathode. During working operation, once a voltage is applied beyond the OLED, electrons flow over the

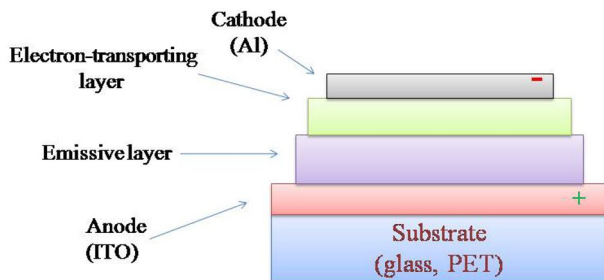


Fig. 9 General schematic representation of organic light emitting diode (OLED) structure

device from the cathode to the anode. The electrons jump into the LUMO level of the organic layer next to the cathode layer from a reserve from the HOMO at the anode side. Recently, this method has also called for the injection of electron holes. The electrons and holes are brought towards each other by electrostatic forces, and recombine to develop an exciton [51]. The working principle of an OLED is shown schematically in Fig. 9.

2.7.2 Photovoltaic Device

Organic semiconductors have enormous potential for the economical production of high numbers of photovoltaic cells. The first photoconductive polyaromatic molecule was discovered at the beginning of the twentieth century [52]. Even though several of these moieties were not stable, they prompted much investigation aimed at improving the charge transport electronic behavior of these conjugated moieties. The first organic solar cell was fabricated on a single organic layer sandwiched in between two metal-based electrodes to carry out the work function. These devices and systems exhibited very poor power conversion efficiency because of low charge carrier formation and inadequate charge transport. Compared to their inorganic counterparts, organic semiconductors have many advantages [53]. Previously, monocrystalline silicon materials were used for solar cells. Production of these types of solar cells production was costly and energy consumption is quite high during fabrication. Nowadays, silicon solar cells have been superseded by organic solar cells because of low production costs, efficiency, inkjet printing, durability, lightweight nature, flexibility and roll-to-roll processing [54, 55]. Moreover, organic semiconductor films can absorb the majority of incident photons due to the high absorption coefficient. The optical and electrochemical band gap of organic conjugated polymers (semiconductors) can be decreased by modifying the chemical structure of the polymer, thereby controlling the absorption spectrum of the photovoltaic cell, and increasing solar cell efficiency.

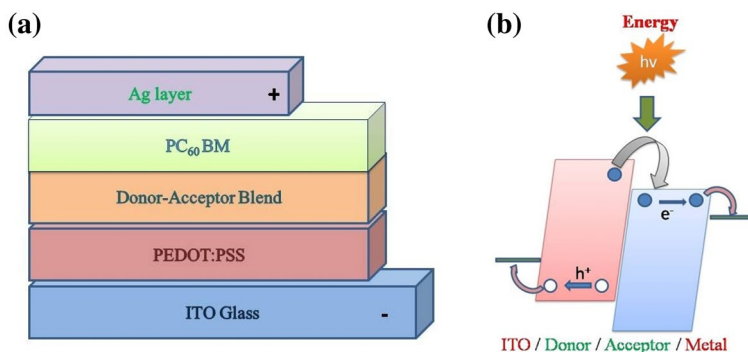
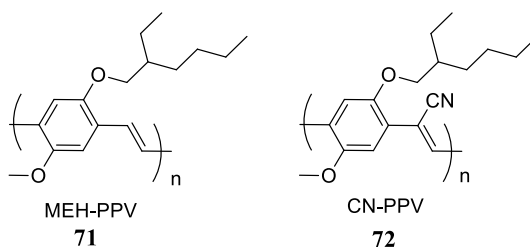


Fig. 10 **a** Schematic representation of bulk heterojunction (BHJ) solar cell. **b** Band gap diagram displaying the hole generation and transport between two electrodes

Fig. 11 Structures of poly[2-methoxy, 5-(2-ethylhexyloxy)-1,4-phenylene vinylene] (MEH-PPV) and cyano-poly(phenylene vinylene) (CN-PPV) polymers



2.7.3 Device Structure

The most general structure and schematic architecture of bulk heterojunction (BHJ) solar cells are shown in Fig. 10a. In solar cell geometry, the bottom electrode is the ITO electrode bearing a negative charge, and the top positive electrode is the metal cathode. On top of the ITO electrode, a conductive PEDOT: PSS polymer is deposited to lessen the roughness of the ITO plate. Then, the BHJ polymer layer is deposited through a solution processing method. This BHJ layer is composed of donor and acceptor materials. Moreover, a phenyl- C_{60} -butyric acid methyl ester ($PC_{60}BM$) layer is deposited between the photoactive layer (BHJ layer) and the metal cathode, this layer acts as an electron acceptor [56].

2.7.4 Photovoltaic Conversion Process

The photovoltaic conversion process is shown in Fig. 10b. In its simplest form, when light passes through ITO glass and touches upon the BHJ (photoactive) layer, electrons jump from the valence band to the conduction band of the semiconducting material followed by generating a hole in the valence bond. The generated charges (exciton) are then passed to the metal electrode by an internal electric field. Once the excitons reach the metal electrode, they dissociated into free electrons and pass through an external power circuit, therefore generating electrical current. Excitons carrying an internal electric field are usually generated by either a $p-n$ junction in

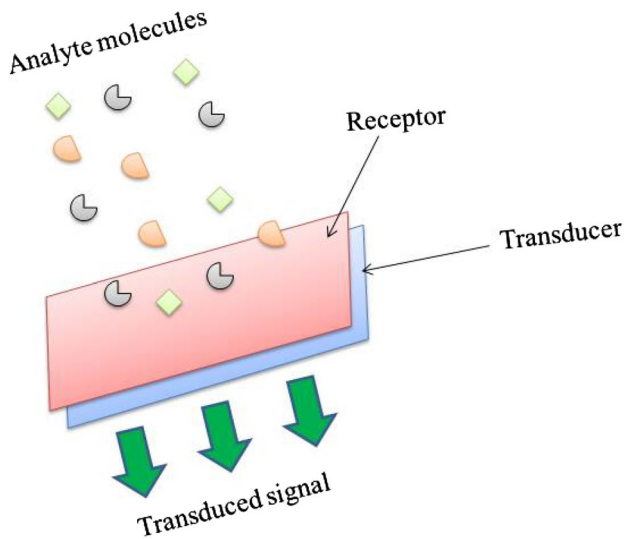


Fig. 12 Schematic representation of the basic sensor system

the BHJ active layer, or by a difference in the work function of both electrodes. Initially, the polymer–polymer solar cell (BHJ) was reported in 1995 [57]. New conjugated polymers have improved the open circuit voltage and efficiency of solar cells by linking an alkyl thiophene side chain (PCE: 8.42–9.58%) [58–60] with fullerene substituents (PCE: > 14%) [61]. Individually fabricated BHJ solar cells now have a composition of poly[2-methoxy, 5-(2-ethylhexyloxy)-1,4-phenylene vinylene] (MEH–PPV) (**71**) and cyano-poly(phenylene vinylene) (CN–PPV) (**72**) (Fig. 11). A polymer thin film is formed through spin casting from the polymer solution. Guo et al. discovered that photoinduced charge transfer occurs between the two polymers [61]. They found low device efficiency at 0.9%, and further improved efficiency in consequent bilayer devices. The low efficiency of the device (observed as 2.0 eV) was due to the high electrical band gap. Higher electrical band gap polymers were capable of absorbing a wide range of the solar spectrum. For example, the polymer poly(heteroarylene-vinylene) showed threefold higher power conversion efficiency with higher short-circuit current. The manageable solar cell efficiency value was calculated as 0.6% [62]. The indacenodithiophene–benzothiadiazole based polymer solar cell showed a greater short-circuit value (9.85 mA cm^{-2}) due to the high hole mobility and wide photo-electronic response. A good power conversion efficiency of 4.52% was attained by the polymer and PC₇₁BM composite [63].

2.7.5 Sensors Based on Conjugated Polymers

A device that observes a signal in the presence of an external substance (i.e., analyte) is called as a sensor. That signal generally depends upon the quantity, magnitude, and strength of the analyte. Generally, the ideal sensor consists of an active layer for detecting the analyte molecules and generates a signal from the transducer

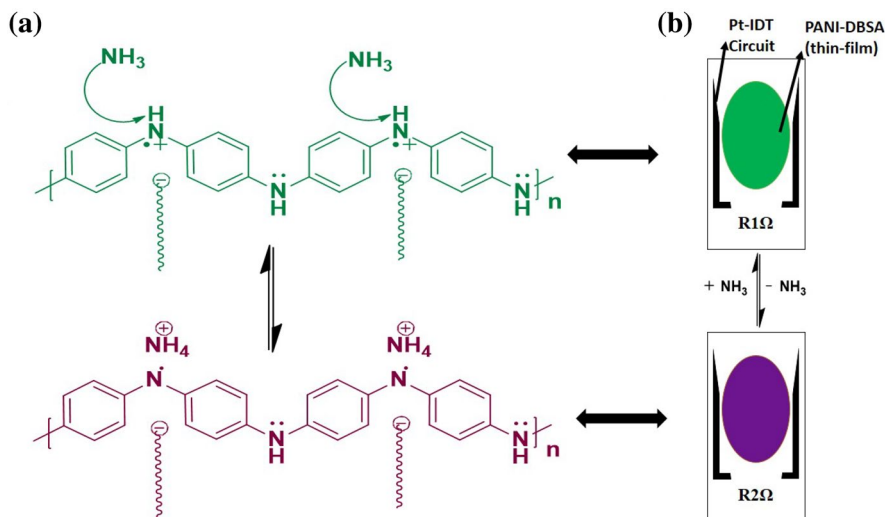


Fig. 13 **a** Reaction of ammonia with polyanilines (PANI). **b** Spin-coated PANI film deposited on the interdigitated platinum electrode, above (*green*) and below (*purple*) is exposure to NH_3 with respect to resistance changes

(Fig. 12). Signal behavior and intensity depend on the surface of active layer and the nature of the analyte. The absorbed signals may be optical or electronic properties of the receptor (active layer). The ideal sensor is a cost-effective, convenient, foolproof device that responds with great and rapid selectivity to a peculiar target biological or chemical material (analyte). Sensor active layers have been achieved by conjugated conducting polymers such as polythiophene, polypyrroles, polyanilines and their derivatives. In recent years, traditional sensors (metal oxide) have been replaced by conjugated polymer-based sensors due to their enhanced characteristics such as immediate response time and better sensitivity at ambient temperature.

In the past 20 years, conjugated polymers have been researched by many scientists worldwide and applied in numerous organic electronic devices [64]. Conjugated polymers have excellent sensor properties and display high sensitivity in chemical and biological target molecules. Chemical sensors based on conjugated polymers provide benefit because spectral changes such as absorption and fluorescence shifts are caused by conformational changes in polymer backbone upon interacting with particular ions. The selectivity and sensitivity of conjugated polymers is related to the intrinsic molecular structure of the polymer backbone, which in turn is dependent on the side chains. For example, Huang's group determined how the side chain properties of cationic conjugated polymers had a significant impact on their complex arrangement with DNA [65]. In 2011, a monopyridyl-based conjugated polymer was used successfully to sense silver cation [66].

Fig. 14 Structure of ammonia gas sensing diketopyrrolopyrrole-(DPP)-based polymer

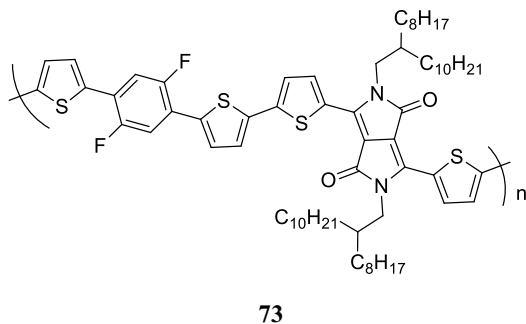


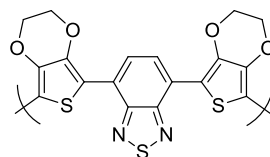
Fig. 15 Schematic representation of a bio-sensing system

2.7.6 Gas Sensors

Among conjugated polymers, polyanilines (PANI) are an extremely important class of sensors due to reversible doping or undoping through protonation or deprotonation. Notable responses in optical and electrochemical properties are observed after exposure of PANI to gases like ammonia, carbon dioxide, nitrogen dioxide or acidic solutions. For example, dodecylbenzene sulfonic acid (DBSA)-doped polyaniline (active layer) senses ammonia gas through its DBSA undoping. Therefore, the resistance of preliminary doped PANI film is higher than ammonia-induced undoping (Fig. 13). Moreover, the level of ammonia doping also displays changes in optical properties; the green color of the polymer film changes markedly to a purple color through its absorption spectrum variation. Compared to traditional inorganic materials, conjugated polymers exhibit enormous advantages, such as tunable electrical properties, optical properties, solution processability, room temperature operation, molecule structure flexibility, high sensitivity, low density, stable performance, good selectivity, rapid response, and recovery.

Diketopyrrolopyrrole (DPP) acceptor based conjugated conductive polymer (**73**) (Fig. 14) includes difluoro phenylene dithiophene and thiophene as donors for the active layer of organic field-effect transistors. The synthesized polymer can successfully sense ammonia gas. It exhibits high sensitivity towards 1000 ppm of ammonia gas by a reliable and gradual negative shift in the transfer curve [67].

Fig. 16 Structure of glucose oxidase enzyme sensed benzo-thiadiazole-based polymer



74

2.7.7 Biosensors

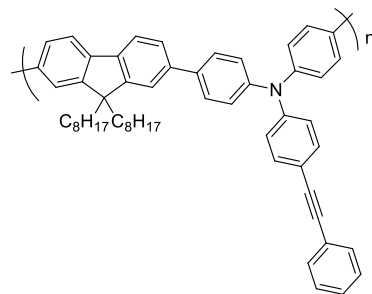
Conjugated polymers have also been significant and well recognized in the sensing of biological compounds. A schematic representation of a bio-sensing system is shown in Fig. 15. Conjugated polymers can make the conjugation with biological molecules due to their bioactivity or biological significance. The conjugated polymers and their blends have developed as capable candidates for high-performance biosensing applications, such as the quantitative detection of substrates like glucose, triglyceride, hydrogen peroxide, cholesterol, DNA, urea, gonorrhoea and other species. Present, many biomaterials, including DNA, RNA, enzymes, antibodies, antigens, amino acids, proteins, and enzymes have been incorporated into conjugated polymer matrices to generate biologically active systems. Hybrid systems (HYBs) consisting of biological molecules have been used as sensors and actuators. The different enzymes have been attached directly or included in the conjugated system as dopants. Enzyme activity is dependent mainly upon the potential value of the conducting polymer, which can be applied to modulate enzyme activity [68]. Interestingly, an electronic tongue consists of six types of sensing units such as stearic acid, polypyrrole, a PANI oligomer, and a mixture of polypyrrole and PANI, has been developed; such sensing systems can distinguish between bitter, sweet, salt, bitter and acidic nature using an electrical impedance measurement [69].

The benzothiadiazole based polymer (74) is a convenient sensor for the glucose oxidase enzyme due to the high electron affinity of the benzothiadiazole unit (Fig. 16). The oxygen level is decreased after the enzymatic reaction of glucose oxidase, which is a monitor at -0.7 V vs Ag/AgCl (3.0 M KCl). The biosensor is characterized by numerous parameters such as kinetic parameters, storage and operational stability [70].

2.7.8 Metal Ion Sensing of Conjugated Polymer

A chemosensor is a chemical sensors sensing particular analyte molecules. Each unique molecule acts as a one chemical sensor device. The chemosensor molecule may detect one or more elements. Occasionally, one component of the molecule can sense two or many elements. Fluorescence is an optical property of a molecule, and is defined as the relaxation of an electron from a higher energy state to the ground state. Changes in the fluorescence signal are generally called fluorescence chemosensors. Recently fluorescent chemosensors have attracted interest in different areas due to their ease of measurement, high sensitivity, and selectivity. Fluorescent

Fig. 17 Structure of Hg^{2+}/Γ^- sensed triphenylamine-based conjugated polymer



75

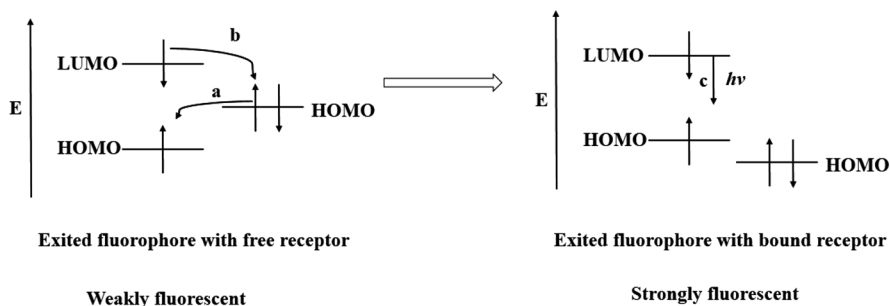


Fig. 18 Energy diagram of fluorescence “turn-on” process of photoinduced electron transfer before and after cation binding

chemosensors are generally built from up to three components: a receptor, fluorophore, and spacer. Of these, the spacer is not responsible for fluorescent signal transduction. In the readout process, the signal may show the changes in fluorescence intensity or emission wavelength. The main advantage of the fluorescent chemosensor is rapid signal observation, which allows real-space and real-time detection of an analyte.

The triphenylamine and fluorene-based conjugated polymer (**75**) is synthesized through a Suzuki coupling reaction (Fig. 17). Fluorescence intensity is markedly decreased by the introduction of Γ^- . The visual apparent color changes from colorless to light yellow. The detection limit of Γ^- is calculated as 2.9×10^{-7} M. Surprisingly, the fluorescence emission of polymer/ Γ^- complex was regained rapidly with the presence of Hg^{2+} . This type of sensor is known as a dual channel sensor. The detection limit of Hg^{2+} is 2.4×10^{-7} M obtained by polymer/ Γ^- complex [71].

2.7.9 Mechanism of Analyte Detection

Fluorescent sensing consists of two main types of mechanism:

1. Photoinduced electron transfer (PET)

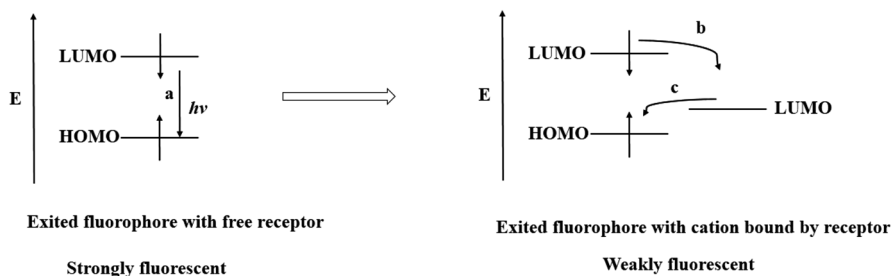


Fig. 19 Energy diagram of fluorescence “turn-off” process of photoinduced electron transfer before and after cation binding

2. Electron energy transfer (EET).

These two mechanisms have been used widely and extensively in designing chemosensors. Fluorescence intensity is altered by both these mechanisms.

2.7.10 Photo-Induced Electron Transfer

There are two categories of photoinduced electron transfer mechanism. One is fluorescence “turn-on” property; the second is fluorescence “turn-off” property upon binding cation. The receptors of fluorescence “turn-on” sensors contain a nonbonding and high energy electron pair. These electrons quench the fluorophore in the absence of analyte through a rapid intramolecular electron transition between the receptor and excited fluorophore (Fig. 18).

The HOMO level of the receptor is lowered due to the coordination between the electron pair and Lewis acid cations in the presence of a solvent. This causes a lower HOMO level and mobilizes the photoinduced electron transfer process, which effectively turns on the fluorescence.

Sometimes, the receptor may also be involved diffusely in a photophysical process. In this process, the LUMO energy level of the cation lies between the HOMO and LUMO energy levels of the fluorophore. The nonradiative process is raised when the cation binds to the receptor. The resulting fluorescence is changed to turn-off after sensing, as shown in Fig. 19.

In both mechanisms, the photoinduced electron transfer process takes place either before or after cation binding. In a fluorescence “turn-on” sensor, the PET process is determined by the HOMO / LUMO level of the fluorophore and the HOMO level of the receptor before cation binding. In a fluorescence “turn-off” process, the PET process affects the HOMO / LUMO level of the fluorophore and the LUMO level of the cation following complex formation.

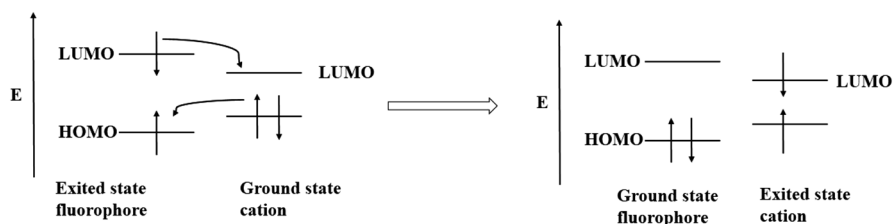


Fig. 20 Orbital energy diagram of double-electron exchange energy transfer (Dexter) mechanism among the excited fluorophore and cation

2.7.11 Electron Energy Transfer

An electron energy transfer process occurs in an excited state alternative to the ground state. This is also a different fluorescence quenching mechanism upon cation binding. There are two types of electron energy transfer mechanism:

- (1) Double electron exchange energy transfer (Dexter).
- (2) Dipole–dipole coupling energy transfer.

Of the two, the Dexter energy transfer arises between fluorophore and the cation system, as shown in Fig. 20. In this system, the fluorophore reached its ground state energy level through a non-radiative decay path. Mainly, the Dexter energy transfer is needed to have convenient contact between the cation and fluorophore with shortest orbital overlap. This kind of fluorescence quenching process requires a suitable energy level between the fluorophore and the cation. A spacer is also required to maintain a short distance and flexibility between the donor and acceptor of the fluorophore.

Conjugated polymers exhibit fluorescence due to their conjugation, and that fluorescence depends on the direct response to various metal ions. So, conjugated polymers can be used precisely as fluorescent sensors. The sensitivity and unique properties of fluorescent conjugated polymers afford new hopes for sensory system evolution. Some conjugated fluorescent sensors showed conformational changes in the polymer backbone due to interaction with the analyte. For example, poly[3-oligo(oxyethylene)-4-methylthophene] exhibits fluorescence changes after interaction with alkali metals, and the fluorescence response is dependent upon the alkali metal concentration [72].

2.7.12 Fluorescence “Turn-Off” Conjugated Polymers

Environmental pollution has developed as a major problem due to hasty industrialization and urbanization. Many chemical industries, such as battery manufacturing, electroplating, tanning, mining, textile manufacturing, automotive, fertilizer manufacturing, coal industries, release different concentrations of heavy metals like copper, cadmium, nickel, silver, lead, etc. The Environmental Protection Agency

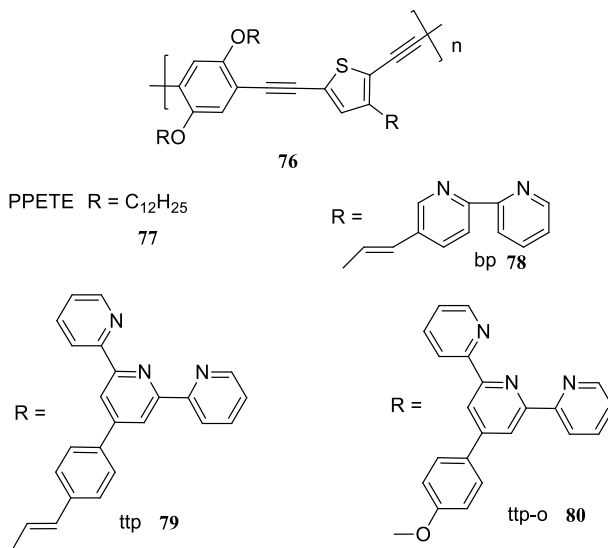


Fig. 21 Structures of the different oligo-pyridine groups and poly[*p*-(phenyleneethynylene)-*alt*-(thienylene ethynylene)] polymer

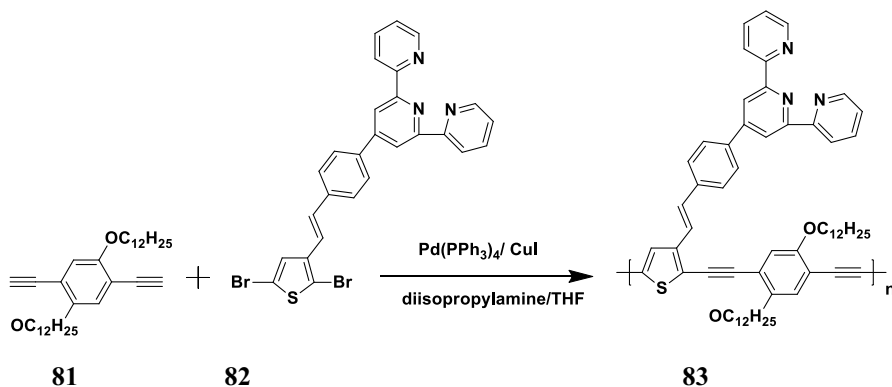


Fig. 22 Synthetic route of polymer 83

declared 13 transition metals to be causing more pollution. These metal ions are persistent in the environment and non-degradable. Heavy metal ion toxicity is known to cause severe health problems, like allergies, premenstrual syndrome, anemia, anorexia, Parkinson’s disease, depression, migraine and many others. So, due to their low cost, rapid detection, selectivity, and sensitivity, there is great demand for improvement of fluorescence-based conjugated polymer sensors for metal cations. Among organic ligands, pyridyl ligands (Lewis bases) can coordinate with a greater number of transition metal ions. For example, different oligopyridine groups and

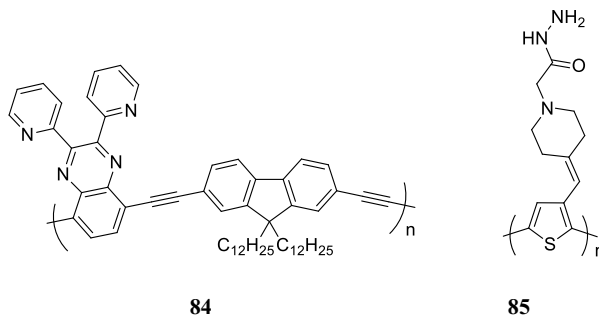


Fig. 23 Structures of fluorescence turn-off based conjugated polymers

poly[*p*-(phenylene ethynylene)-*alt*-(thienylene ethynylene)] polymer (**76**) acts as a transition metal receptor [73] as shown in Fig. 21.

This combination of polymer and pyridine ligands (**78–80**) exhibits a highly luminescence nature due to strong conjugation. The Lewis base (pyridine multi-dentate) together with polyarylene ethynylene acts as an excellent chemosensor for highly toxic transition metals. Among all pyridine ligands, tolylterpyridine (**79**) ligand based polymer showed maximum fluorescence quenching and sensitivity towards metal cations. This is due to the greater distance between receptor (**79**) and polymer backbone, which may develop energy transfer and improve cation quenching sensitivity and selectivity [69].

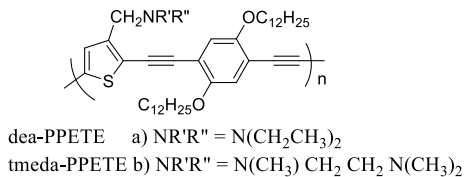
Polymer **83** was cross-coupled from the monomers of 1,4-diethynyl-2,5-didodecyloxybenzene (**81**) and aryl halide (**82**) in the presence of Pd-catalyst (Fig. 22). The long dodecyloxy chains of the compound improve the solubility of the polymer. The tolylterpyridine ligand-receptor was inserted into the thiophene moiety by the Horner-Wittig-Emmons reaction [74]. Due to the different chelating nature of terpyridine with various transition metals, the synthesized polymer displayed excellent selectivity towards different metal cations such as Cd²⁺, Cr⁶⁺, Mn²⁺, and Ni²⁺. Polymer (**83**) and metal concentration were maintained at 3.08 μm and 1.54 μm, respectively. Polymer **83** successfully quenched the 29% fluorescence intensity of Ni²⁺, 79.6% fluorescence intensity of Cd²⁺, and quenching was not recognized in the presence of remaining metal cations such as Ca²⁺, Pb²⁺, Na²⁺ and Hg²⁺.

Stern-Volmer analysis was used to recognize the quenching nature of polymer **83**. Different types of molecular interactions can be observe in quenching. The collisional interaction among the quencher and fluorophore is called dynamic or collisional quenching. Collisional quenching can be characterized by the Stern–Volmer equation.

$$\frac{I_0}{I} = \frac{\tau_0}{\tau} = 1 + k_q \tau_0 [Q]$$

where, I_0 =primary fluorescence emission intensity in the absence of quenchers; I =fluorescence intensity; K_q =rate constant of collisional quenching;

Fig. 24 Structure of fluorescence turn-on poly[*p*-(phenylene ethylene)-*alt*-(thienylene ethylene)] (fluorophore) (PPETE) based conjugated polymer



86

τ_0 = fluorophore lifetime in the absence of quencher; τ = fluorescence lifetime in the presence of quencher; $[Q]$ = concentration solution of quencher.

Quenching takes place between quencher and fluorophore, which results in a non-fluorescence complex—this is called static quenching. In this type of quenching, fluorescence intensity is reduced and explored by the following Stern–Volmer equation.

$$\frac{I_0}{I} = 1 + K_{SV}[Q]$$

where, I_0 = original fluorescence intensity of polymer; I = final fluorescence intensity of polymer after metal binding; K_{SV} = Stern-Volmer quenching constant; $[Q]$ = quencher (metal ion).

The Stern-Volmer quenching constant of $83 + \text{Ni}^{2+}$ was calculated as 5.0×10^{-6} M. The results suggesting that static quenching is mainly raised as a complexation process rather than as dynamic quenching. Among Co^{2+} , Cr^{6+} , Cu^{2+} , Fe^{2+} , Zn^{2+} , Ni^{2+} , and Mn^{2+} metal ions, Ni^{2+} showed a capable response with polymer **83**.

The 2,3-di(pyridine-2yl)quinoxaline and fluorene-based conjugated polymer (**84**) was synthesized via the Sonogashira coupling reaction (Fig. 23). The synthesized polymer has high selectivity and sensitivity towards silver ion. The visual green color is changed to brown-red color and green fluorescence intensity is quenched by 85%. The detection limit of Ag^+ is 5×10^{-7} mol L⁻¹, which is an adequately low detection limit at a sub-millimolar concentration [75].

Water-soluble thiophene and hydrazide based polymer (**85**) acts as an excellent sensing probe for Cu^{2+} and Hg^{2+} in water media (Fig. 23). The fluorescence intensity of **85** is decreased upon addition of Cu^{2+} and Hg^{2+} ions due to complex formation. Other metal cations did not cause serious fluorescence emission changes. After binding with Cu^{2+} and Hg^{2+} ions, the yellow color fluorescence of the polymer is completely quenched. The detection limits for Cu^{2+} and Hg^{2+} were calculated to be 2.0×10^{-10} M and 2.0×10^{-9} M, respectively.

2.7.13 Fluorescence “Turn-On” Conjugated Polymers

The fluorescence quenching (turn-off) process has been widely reported in the literature, but there are few reports on fluorescence turn-on process towards metal cations. Turn-on fluorescence sensors have the enormous advantage of ease of measurement at low concentration with a dark background. Fluorescent polymers with “turn-on” capability are due to photoinduced electron transfer [76]. For example,

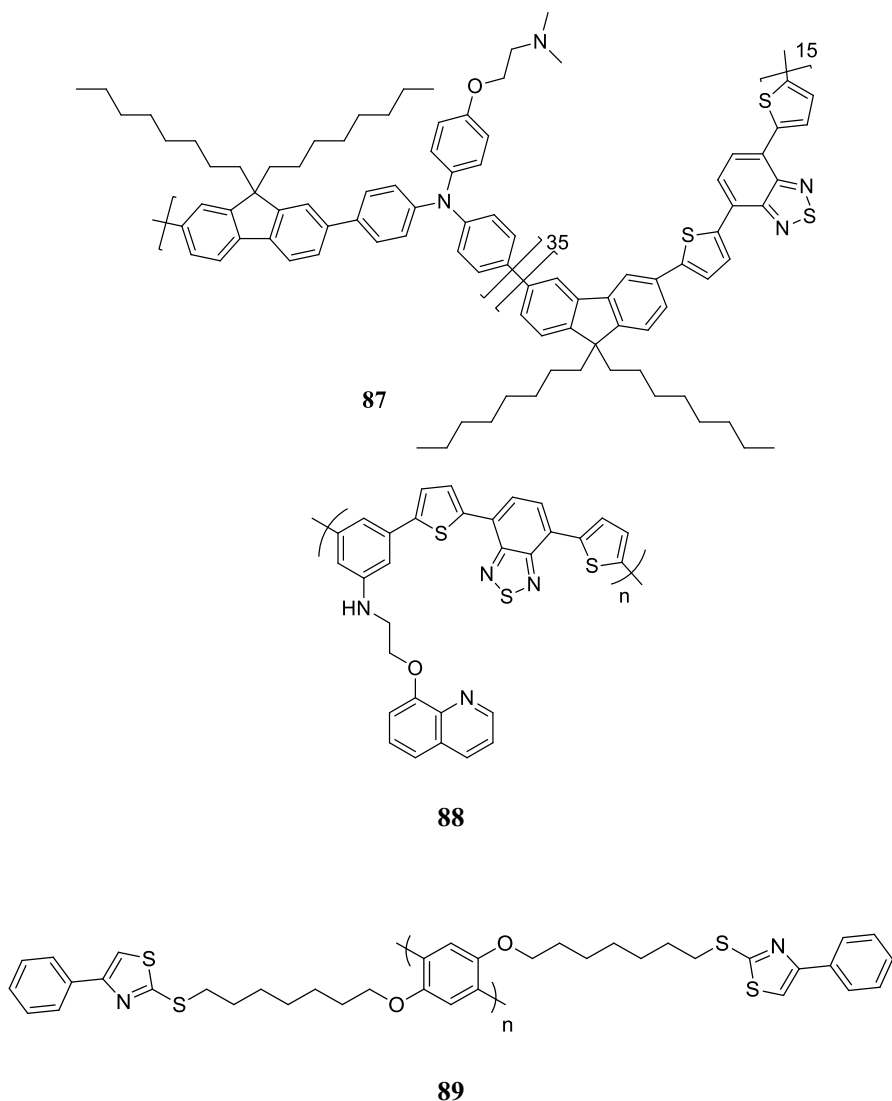


Fig. 25 Structures of various fluorescence turn-on based conjugated polymers

poly[*p*-(phenylene ethylene)-*alt*-(thienylene ethynylene)] (fluorophore) (PPETE) (**86**) (Fig. 24) and various amino groups (receptors) act as a fluorescence “turn-on” polymers. These polymers are synthesized through the palladium-based cross-coupling reaction [77].

Among both polymers, **86b** exhibited various fluorescence “turn-on” properties in the presence of a greater number of cations. Polymer **86a** displayed a partial fluorescence “turn-on” effect with metal cations. The different nature of these two conjugated polymers could be due to two effects: (1) the photoinduced electron transfer

due to amino groups, which have different energy levels before cation binding; (2) the greater equilibrium constant for cation binding, which could also be the reason for the increased fluorescence-enhancing nature of polymer **86b**. Among all transition metals, Ca^{2+} , Zn^{2+} , and Hg^{2+} show extra fluorescence intensity changes. The fluorescence enhancement of three metal ions is saturated at an early stage ($\sim 5 \mu\text{M}$) when the receptor concentration is close to the cation concentration. For **86b**, the selectivity and sensitivity nature of Ca^{2+} , Zn^{2+} , and Hg^{2+} ions have been investigated intensively and systematically [77]. The polymer in tetrahydrofuran is treated with several metal ions, such as Li^+ , Na^+ , K^+ , Mg^{2+} , Mn^{2+} , Fe^{2+} , Co^{2+} , Ni^{2+} , Cu^{2+} , and Cd^{2+} , in addition to Ca^{2+} , Zn^{2+} , and Hg^{2+} ions. Most cations increased the fluorescence intensity of **86b**.

Another example is triphenylamine and the sulfur-containing (thiophene, benzothiadiazole) red-emitting conjugated polymer (**87**), which acts as an excellent optical probe for the detection of I^- and Hg^{2+} ions (Fig. 25) [78]. The fluorescent nature of the polymer is drastically quenched by I^- addition and the visual color of the polymer solution is changed from pale pink to yellow accordingly. The color change of polymer solution is clearly observed by the naked eye, so it is called a colorimetric probe. The iodine detecting polymer solution was established by competing experiments toward different anions with a detection limit of 2.3×10^{-7} M. Absorption and fluorescence curves of **87**/ I^- were regained quickly with the addition of Hg^{2+} ions, due to the strong affinity between Hg^{2+} and I^- . The detection limit of Hg^{2+} ions was calculated as 1.1×10^{-7} M from **87**/ I^- . The entire experiment suggests that synthesized polymer **87** can act as a dual sensor, and is a highly selective and sensitive probe for I^- and Hg^{2+} ions.

Polymer **88** has good selectivity and sensitivity towards Hg^{2+} ions with notable “turn-on” fluorescence (Fig. 25). The polymer has a weak fluorescence in DMSO solution due to photoinduced electron transfer from electron-donating groups (OH, NH_2) to electron-withdrawing groups. When introducing different metal ions into the polymer solution, an obvious fluorescence enhancement was observed only in the presence of Hg(II) ions. The blue color emission of polymer **88** is changed to red in the presence of Hg(II) ions. The fluorescence intensity of the polymer solution is gradually increased with the addition of Hg(II) ions from 1.0×10^{-6} M to 1.0×10^{-4} M. The binding constant of the polymer with Hg(II) ions was calculated to be $2.75 \times 10^5 \text{ M}^{-1}$. The result of thermogravimetric analysis revealed that the polymer exhibited good thermal stability (T_d , 228 °C) [79].

The phenylthiazole based conjugated polymer (**89**) is highly selective and sensitive for inorganic Hg^{2+} and I^- salts (Fig. 25). The synthesized polymer exhibits a “turn-off–turn-on” response against I^- and Hg^{2+} ions in seafood samples. The blue color fluorescence of the polymer is quenched by I^- and reappears in the presence Hg^{2+} ions. A colorimetric response is also observed with the polymer. The colorless solution changes to yellow after the addition of I^- salts, which becomes colorless upon addition of Hg^{2+} ions. The detection limit of Hg^{2+} is calculated to be 1.86 nM [80].

3 Conclusion

In this review, we have outlined the background studies, synthesis, properties and applications of some of the key conducting organic polymers that have become significant in recent years. The described optoelectronic properties of conjugated polymers are essential to the understanding of the fundamental electronic structure of these materials. Key optoelectronic factors, such as absorption, emission, solubility, thermal stability, HOMO/LUMO values and energy band gap values, have been discussed with representative examples. Further, choice of donor and acceptor counterparts of polymer also plays significant role for low band gap and solar cell efficiency improvement. Although selection of donor/acceptor combination and altering of band gap conductivity is still currently 'state of the art,' most rules of thumb have been pointed out. Several conjugated polymeric sensory systems for metal cation and anion detection have been discussed in this review. These discussions about sensor systems help us further understand the energy migration and sensing mechanism along these polymer backbones. This research influences sensing behavior and may be helpful for the future design of new classes of chemosensors, as well as for fundamental studies of the electronic properties of semiconducting polymers in confined dimensionalities with attractive applications in the field of optoelectronics.

Acknowledgement The authors would like to acknowledge the VIT University for supporting this work.

References

1. Kushida S, Braam D, Dao TD, Saito H, Shibasaki K, Ishii S, Nagao Y, Cui A, Kuwabara J, Kanbara T, Kijima M, Lorke A, Yamamoto Y (2016) Conjugated polymer blend microsphere for efficient, long range light energy transfer. *ACS Nano* 10:5543–5549
2. Naarmann H (2000) Polymers electrically conducting, *ullmann's encyclopedia of industrial chemistry*
3. Akamatu H, Inokuchi H, Matsunaga Y (1954) Electrical conductivity of the perylene–bromine complex. *Nature* 173(4395):168–169
4. Ferraris J, Cowan DO, Walatka VT, Perlstein JH (1973) Electron transfer in a new highly conducting donor-acceptor complex. *J Am Chem Soc* 95(3):948–949
5. Bolto BA, McNeill R, Weiss DE (1963) Electronic conduction in polymers. III. Electronic properties of polypyrrole. *Aust J Chem* 16(6):1090–1103
6. De Surville R, Jozefowicz M, Yu LT, Pepichon J, Buvet R (1968) Electrochemical chains using protolytic organic semiconductors. *Electrochim Acta* 13(6):1451–1458
7. Shirakawa H, Louis EJ, MacDiarmid AG, Chiang CK, Heeger AJ (1977) Synthesis of electrically conducting organic polymers: halogen derivatives of polyacetylene, (CH)_x. *J Chem Soc Chem Commun* 37:578–580
8. Burroughes JH, Bradley DDC, Brown AR, Marks RN, Mackay K, Friend RH, Holmes AB (1990) Light-emitting diodes based on conjugated polymers. *Nature* 347(6293):539–541
9. Friend RH, Gymer RW, Holmes AB, Burroughes JH (1999) Electroluminescence in conjugated polymers. *Nature* 397(6715):121
10. Holdcroft S (2001) Patterning pi-conjugated polymers. *Adv Mater* 13(23):1753–1765
11. Gierschner J, Cornil J, Egelhaaf HJ (2007) Optical bandgaps of π -conjugated organic materials at the polymer limit: experiment and theory. *Adv Mater* 19(2):173–191
12. Leger JM (2008) Organic electronics: the ions have it. *Adv Mater* 20(4):837–841

13. Hameed S, Predeep P, Baiju MR (2010) Polymer light emitting diodes-a review on materials and techniques. *Rev Adv Mater Sci* 26:30–42
14. Sonar P, Williams EL, Singh SP, Dodabalapur A (2011) Thiophene–benzothiadiazole–thiophene (D–A–D) based polymers: effect of donor/acceptor moieties adjacent to D–A–D segment on photo-physical and photovoltaic properties. *J Mater Chem* 21(28):10532–10541
15. Akpınar HZ, Udum YA, Toppare L (2015) Multichromic and soluble conjugated polymers containing thiazolothiazole unit for electrochromic applications. *Eur Polym J* 63:255–261
16. Fukuda K, Maki I, Ikeda S, Ito S (1993) Microtextures formed by the remelting reaction in belite crystals. *J Am Ceram Soc* 76:2942–2944
17. Wnek EG, Chien JCW, Karasz FE, Lillya CP (1979) Electrically conducting derivatives of poly(*p*-phenylene vinylene). *Polymer* 20:1441–1443
18. Kanazawa KK, Diaz AF, Geiss RH, Gill WD, Kwak JF, Logan JA, Rabolt JF, Street B (1979) Organic metals' polypyrrole a stable synthetic metallic polymer. *Chem Commun* 12:854–855
19. Diaz AF, Logan JA (1980) Electroactive polyaniline films. *J Electroanal Chem Interfacial Electrochem* 111(1):111–114
20. Waltman RJ, Bargon J, Diaz AF (1983) Electrochemical studies of some conducting polythiophene films. *J Phys Chem* 87:1459–1463
21. Heeger AJ (2001) Nobel lecture: semiconducting and metallic polymers: The fourth generation of polymeric materials. *Rev Mod Phys* 73(3):681–700
22. Yamamoto T, Senechika K, Yamamoto A (1980) Preparation of thermostable and electric-conducting poly (2,5-thienylene). *J Polym Sci* 18:9–12
23. Champion RD, Cheng KF, Pai CL, Chen WC, Jenekhe SA (2005) Electronic properties and field-effect transistors of thiophene-based donor–acceptor conjugated copolymers. *Macromol Rapid Commun* 26(23):1835–1840
24. Chen B, Wu Y, Wang M, Wang S, Sheng S, Zhu W, Tian H (2004) Novel fluorene-*alt*-thienylenevinylene-based copolymers: tuning luminescent wavelength via thiophene substitution position. *Eur Polymer J* 40(6):1183–1191
25. Do TT, Ha YE, Kim JH (2013) Effect of the number of thiophene rings in polymers with 2,1,3-benzooxadiazole core on the photovoltaic properties. *Org Electron* 14(10):2673–2681
26. Muhalbacher D, Scharber M, Morana M, Zhu Z, Waller D, Gaudiana R, Brabec C (2006) High photovoltaic performance of a low-bandgap polymer. *Adv Mater* 18(21):2884–2889
27. Sonar P, Singh SP, Leclere P, Surin M, Lazzaroni R, Lin TT, Sellinger A (2009) Synthesis, characterization and comparative study of thiophene–benzothiadiazole based donor–acceptor–donor (D–A–D) materials. *J Mater Chem* 19(20):3228–3237
28. Burroughes JH, Bradley DDC, Brown AR, Marks RN, Mackay K, Friend RH, Holmes AB (1990) Light-emitting diodes based on conjugated polymers. *Nature* 347(6293):539–541
29. Masse MA, Martin DC, Thomas E, Karasz FE, Petermann JH (1990) Crystal morphology in pristine and doped films of poly(*p*-phenylene vinylene). *J Mater Sci* 25(1):311–320
30. Alam MM, Jenekhe SA (2002) Polybenzobisazoles are efficient electron transport materials for improving the performance and stability of polymer light-emitting diodes. *Chem Mater* 14(11):4775–4780
31. Hou J, Yang C, Qiao J, Li Y (2005) Synthesis and photovoltaic properties of the copolymers of 2-methoxy-5-(2'-ethylhexyloxy)-1, 4-phenylene vinylene and 2, 5-thienylene-vinylene. *Synth Met* 150(3):297–304
32. Sanchez CO, Sobarzo P, Gatica N (2015) Electronic and structural properties of polymers based on phenylene vinylene and thiophene units. Control of the gap by gradual increases of thiophene moieties. *New J Chem* 39(10):7979–7987
33. Wong WY, Wang XZ, He Z, Chan KK, Djurišić AB, Cheung KY, Chan WK (2007) Tuning the absorption, charge transport properties, and solar cell efficiency with the number of thienyl rings in platinum-containing poly (aryleneethynylene) s. *J Am Chem Soc* 129(46):14372–14380
34. Zhang M, Fan H, Guo X, He Y, Zhang Z, Min J, Zhang J, Zhao G, Zhan X, Li Y (2010) Synthesis and photovoltaic properties of bithiazole-based donor-acceptor copolymers. *Macromolecules* 43(13):5706–5712
35. Zhou E, Cong J, Wei Q, Tajima K, Yang C, Hashimoto K (2011) All-polymer solar cells from perylene diimide based copolymers: material design and phase separation control. *Angew Chem Int Ed* 50(12):2799–2803
36. Havinga EE, Ten Hoeve W, Wynberg H (1993) Alternate donor–acceptor small-band-gap semiconducting polymers; Polysquaraines and polycroconaines. *Synth Metals* 55(1):299–306

37. Kitamura C, Tanaka S, Yamashita Y (1996) Design of narrow-bandgap polymers: syntheses and properties of monomers and polymers containing aromatic-donor and *o*-quinoid-acceptor units. *Chem Mater* 8(2):570–578
38. Jayakannan M, Van Hal PA, Janssen RA (2002) Synthesis and structure-property relationship of new donor–acceptor-type conjugated monomers and polymers on the basis of thiophene and benzothiadiazole. *J Polym Sci Part A Polym Chem* 40(2):251–261
39. Sivula K, Luscombe CK, Thompson BC, Fréchet JM (2006) Enhancing the thermal stability of polythiophene: fullerene solar cells by decreasing effective polymer regioregularity. *J Am Chem Soc* 128(43):13988–13989
40. Zhou H, Yang L, You W (2012) Rational design of high performance conjugated polymers for organic solar cells. *Macromolecules* 45(2):607–632
41. Son HJ, He F, Carsten B, Yu L (2011) Are we there yet? Design of better conjugated polymers for polymer solar cells. *J Mater Chem* 21:18934–18945
42. Keshotov ML, Sharma GD, Kochurov VS, Khokhlov AR (2013) New donor–acceptor conjugated polymers based on benzo[1,2-b:4,5-b']dithiophene for photovoltaic cells. *Synth Met* 166:7–13
43. Karpagam S, Guhanathan S (2014) Emitting oligomer containing quinoline group: synthesis and photophysical properties of conjugated oligomer obtained by Wittig reaction. *J Lumin* 145:752–759
44. Vishnumurthy KA, Sunitha MS, Philip R, Adhikari AV (2011) New diphenylamine-based donor–acceptor-type conjugated polymers as potential photonic materials. *React Funct Polym* 71(12):1119–1128
45. Upadhyay A, Karpagam S (2017) Synthesis and photo physical properties of carbazole based quinoxaline conjugated polymer for fluorescent detection of Ni²⁺. *Dyes Pigm* 139:50–64
46. Ammar KB, Guergouri M, Mosbah S, Bencharif L (2015) The synthesis, physicochemical properties and electrochemical polymerization of fluorene-based derivatives as precursors for conjugated polymers. *Tetrahedron Lett* 56:2574–2578
47. Huo L, He C, Han M, Zhou E, Li Y (2007) Alternating copolymers of electron-rich arylamine and electron-deficient 2, 1, 3-benzothiadiazole: synthesis, characterization and photovoltaic properties. *J Polym Sci Part A Polym Chem* 45(17):3861–3871
48. Casey A, Ashraf RS, Fei Z, Heeney M (2014) Thioalkyl-substituted benzothiadiazole acceptors: copolymerization with carbazole affords polymers with large stokes shifts and high solar cell voltages. *Macromolecules* 47(7):2279–2288
49. Casey A, Han Y, Fei Z, White AJ, Anthopoulos TD, Heeney M (2015) Cyano substituted benzothiadiazole: a novel acceptor inducing *n*-type behaviour in conjugated polymers. *J Mater Chem C* 3(2):265–275
50. Mikroyannidis JA, Stylianakis MM, Suresh P, Balraju P, Sharma GD (2009) Low band gap vinylene compounds with triphenylamine and benzothiadiazole segments for use in photovoltaic cells. *Org Electron* 10(7):1320–1333
51. Ke L, Chen P, Kumar RS, Burden AP, Chua SJ (2006) Indium-tin-oxide-free organic light-emitting device. *IEEE Trans Electron Devices* 53(6):1483–1486
52. Moore W, Silver M (1960) Generation of free carriers in photoconducting anthracene. I. *J Chem Phys* 33(6):1671–1676
53. Ranjan S, Balaji S, Panella RA, Ydstie BE (2011) Silicon solar cell production. *Comput Chem Eng* 35(8):1439–1453
54. Yang X, Loos J, Veenstra SC, Verhees WJ, Wienk MM, Kroon JM, Janssen RA (2005) Nanoscale morphology of high-performance polymer solar cells. *Nano Lett* 5(4):579–583
55. Krebs FC, Norrman K (2007) Analysis of the failure mechanism for a stable organic photovoltaic during 10,000 h of testing. *Prog Photovoltaics Res Appl* 15(8):697–712
56. Gunes S, Neugebauer H, Sariciftci NS (2007) Conjugated polymer-based organic solar cells. *Chem Rev* 107(4):1324–1338
57. Yu G, Heeger AJ (1995) Charge separation and photovoltaic conversion in polymer composites with internal donor/acceptor heterojunctions. *J Appl Phys* 78(7):4510–4515
58. Cui C, Wong W-Y, Li Y (2014) Improvement of open-circuit voltage and photovoltaic properties of 2D-conjugated polymers by alkylthio substitution. *Energy Environ Sci* 7:2276–2284
59. Cui C, He Z, Wu Y, Cheng X, Wu H, Li Y, Cao Y, Wong W-Y (2016) High-performance polymer solar cells based on a 2D-conjugated polymer with an alkylthio side-chain. *Energy Environ Sci* 9:885–891

60. Yang H, Wu Y, Zou Y, Dong Y, Yuan J, Cui C, Li Y (2018) A new polymer donor for efficient polymer solar cells: simultaneously realizing high short-circuit current density and transparency. *J Mater Chem A* 6:14700–14708
61. Guo B, Li W, Luo G, Guo X, Yao H, Zhang M, Hou J, Li Y, Wong W-Y (2018) Exceeding 14% efficiency for solution-processed tandem organic solar cells combining fullerene and nonfullerene-based subcells with complementary absorption. *ACS Energy Lett* 3:2566–2572
62. Grisorio R, Allegratta G, Romanazzi G, Suranna GP, Mastrorilli P, Mazzeo M, Gigli G (2012) An insight into the potential of random poly(heteroarylene–vinylene)s as donor materials in bulk heterojunction solar cells. *Macromolecules* 45(16):6396–6404
63. Liu D, Sun L, Du Z, Xiao M, Gu C, Wang T, Yang R (2014) Benzothiadiazole—an excellent acceptor for indacenodithiophene based polymer solar cells. *RSC Adv* 4(71):37934–37940
64. Guo X, Baumgarten M, Mullen K (2013) Designing π -conjugated polymers for organic electronics. *Prog Polym Sci* 38(12):1832–1908
65. Huang YQ, Liu XF, Fan QL, Wang L, Song S, Wang LH, Huang W (2009) Tuning backbones and side-chains of cationic conjugated polymers for optical signal amplification of fluorescent DNA detection. *Biosens Bioelectron* 24(10):2973–2978
66. Hu Y, Xiao Y, Huang H, Yin D, Xiao X, Tan W (2011) An anion-conjugated polyelectrolyte designed for the selective and sensitive detection of silver (I). *Chem Asian J* 6(6):1500–1504
67. Jeong SH, Lee JY, Lim B, Lee J, Noh YY (2017) Diketopyrrolopyrrole-based conjugated polymer for printed organic field-effect transistors and gas sensors. *Dyes Pigment* 140:244–249
68. Kane-Maguire LAP, Wallace GG (2001) Communicating with the building blocks of life using organic electronic conductors. *Synth Met* 119(1):39–42
69. Riul A, Soto AG, Mello SV, Bone S, Taylor DM, Mattoso LHC (2003) An electronic tongue using polypyrrole and polyaniline. *Synth Met* 132(2):109–116
70. Emre FB, Ekiz F, Balan A, Emre S, Timur S, Toppare L (2011) Conducting polymers with benzothiadiazole and benzoselenadiazole units for biosensor applications. *Sens Actuators B Chem* 158(1):117–123
71. Ma F, Shi W, Mi H, Luo J, Lei Y, Tian Y (2013) Triphenylamine-based conjugated polymer/ Γ -complex as turn-on optical probe for mercury (II) ion. *Sens Actuators B Chem* 182:782–788
72. Levesque I, Leclerc M (1996) Ionochromic and thermochromic phenomena in a regioregular polythiophene derivative bearing oligo (oxyethylene) side chains. *Chem Mater* 8(12):2843–2849
73. Fan LJ, Zhang Y, Murphy CB, Angell SE, Parker MF, Flynn BR, Jones WE Jr (2009) Fluorescent conjugated polymer molecular wire chemosensors for transition metal ion recognition and signaling. *Coord Chem Rev* 253(3–4):410–422
74. Boutagy J, Thomas R (1974) Olefin synthesis with organic phosphonate carbanions. *Chem Rev* 74(1):87–99
75. Cui W, Wang L, Xiang G, Zhou L, An X, Cao D (2015) A colorimetric and fluorescence “turn-off” chemosensor for the detection of silver ion based on a conjugated polymer containing 2, 3-di(pyridin-2-yl) quinoxaline. *Sens Actuators B Chem* 207:281–290
76. Rurack K, Kollmannsberger M, Resch-Genger U, Daub J (2000) A selective and sensitive fluoroionophore for Hg^{II}, Ag^I, and Cu^{II} with virtually decoupled fluorophore and receptor units. *J Am Chem Soc* 122(5):968–969
77. Fan LJ, Jones WE (2006) A highly selective and sensitive inorganic/organic hybrid polymer fluorescence “turn-on” chemosensory system for iron cations. *J Am Chem Soc* 128(21):6784–6785
78. Shi W, Ma F, Xie Z (2015) Sulfur-containing, triphenylamine-based red-emitting conjugated polymer/ Γ assembly as turn-on optical probe for mercury (II) ion. *Sens Actuators B Chem* 220:600–606
79. Feng L, Deng Y, Wang X, Liu M (2017) Polymer fluorescent probe for Hg(II) with thiophene, benzothiazole and quinoline groups. *Sens Actuators B Chem* 245:441–447
80. Pavase TR, Lin H, Li Z (2015) Rapid detection methodology for inorganic mercury (Hg²⁺) in sea-food samples using conjugated polymer (1,4-bis-(8-(4-phenylthiazole-2-thiol)-octyloxy)-benzene) (PPT) by colorimetric and fluorescence spectroscopy. *Sens Actuators B Chem* 220:406–413